

17. Fülöp, V., Moir, J. W. B., Ferguson, S. J. & Hajdu, J. Crystallisation and preliminary crystallographic study of cytochrome *cd*, nitrite reductase from *Thiosphaera pantotropha*. *J. Mol. Biol.* **232**, 1211–1212 (1993).
18. Berger, H. & Wharton, D. C. Small angle X-ray scattering studies of oxidised and reduced cytochrome oxidase from *Pseudomonas aeruginosa*. *Biochim. Biophys. Acta* **622**, 355–359 (1980).
19. Moore, G. R. & Pettigrew, G. W. *Cytochromes c: Evolutionary, Structural and Physicochemical Aspects* (Springer, Berlin, 1990).
20. Pettigrew, G. W. & Moore, G. R. *Cytochromes c: Biological Aspects* (Springer, Berlin, 1987).
21. Harutunyan, E. H. *et al.* The binding of carbon monoxide and nitric oxide to leghaemoglobin in comparison with other haemoglobins. *J. Mol. Biol.* **264**, 152–161 (1996).
22. Edwards, S. L., Kraut, J. & Poulos, T. L. Crystal structure of nitric oxide inhibited cytochrome-c peroxidase. *Biochemistry* **27**, 8074–8081 (1988).
23. Adman, E. T., Godden, J. W. & Turley, S. The structure of copper nitrite reductase from *Achromobacter cycloclastes* at five pH values, with NO<sub>2</sub> bound and with type II copper depleted. *J. Biol. Chem.* **270**, 27458–27474 (1995).
24. Williams, P. A. thesis, Oxford Univ. (1996).
25. Poulos, T. L. Ligands and electrons and haem proteins. *Nature Struct. Biol.* **3**, 401–403 (1996).
26. Wittung, P. & Malmstrom, B. G. Redox-linked conformational changes in cytochrome *c* oxidase. *FEBS Lett.* **388**, 47–49 (1996).
27. Pascher, T., Chesick, J. P., Winkler, J. R. & Gray, H. B. Protein folding triggered by electron transfer. *Science* **271**, 1558–1560 (1996).
28. Kraulis, P. J. MOLSCRIPT: a program to produce both detailed and schematic plots of protein. *J. Appl. Crystallogr.* **24**, 946–950 (1991).
29. Merritt, E. A. & Murphy, M. E. P. Raster3D Version 2.0. A program for photorealistic molecular graphics. *Acta Crystallogr. D* **50**, 869–873 (1994).
30. Brünger, A. T. The free *R* value: a novel statistical quantity for assessing the accuracy of crystal structures. *Nature* **355**, 472–474 (1992).

**Acknowledgements.** We thank the ESRF and SRS Daresbury for data collection facilities; the EMBL outstation, Grenoble, for use of an image plate detector; M.L.D. Page for expert advice; R. Bryan and R. Esnouf for computing; K. Harlos for help with in-house data collection; F. Armstrong and J. Hirst for providing electrochemically reduced methyl viologen. This work was supported by MRC, BBSRC and EU-BIOTECH. The Oxford Centre for Molecular Sciences is funded jointly by BBSRC, EPSRC and MRC. N.E.W.S. was supported by a Wellcome Trust prize studentship. V.F. is a Royal Society university research fellow.

Correspondence and requests for materials should be addressed to P.A.W. (e-mail: pamela@scripps.edu), V.F. (e-mail: vilmos@biop.ox.ac.uk) or J.H. (e-mail: janos@xray.bmc.uu.se).

## errata

### The yeast genome directory

*Nature* **387** (suppl.) (1997)

In the list of authors given on page 5 of this supplement, the names of some authors were omitted or misspelled (asterisks). These were: R. Altmann; W. Arnold\*; M. de Haan\*; K. Hamberg; K. Hinni; L. Jones; W. Kramer; H. Küster\*; K. C. T. Maurer\*; D. Niblett; N. Paricio\*; A. G. Parle-McDermott\*; C. Rebuschung; C. Richards; L. Rifkin\*; J. Robben; C. Rodrigues-Pousada\*; I. Schaaff-Gerstenschläger\*; P. H. M. Smits\*; Y. Su\*; Q. J. M. van der Aart\*; J. C. van Vliet-Reedijk\*; A. Wach; M. Yamazaki\*. □

### Measurements of elastic anisotropy due to solidification texturing and the implications for the Earth's inner core

Michael I. Bergman

*Nature* **389**, 60–63 (1997)

Owing to a typographical error, this Letter appeared under the title "Measurements of electric anisotropy due to solidification texturing and the implications for the Earth's inner core". The word 'elastic' in the first line was erroneously replaced with 'electric'. □

### cAMP-induced switching in turning direction of nerve growth cones

Hong-jun Song, Guo-li Ming & Mu-ming Poo

*Nature* **388**, 275–279 (1997)

The order of panels in Fig. 3 of this Letter is incorrect as published. Figure 3a–e should be labelled as f–j, and Fig. 3f–j should be labelled a–e. □

## corrections

### Synthesis and X-ray structure of dumb-bell-shaped C<sub>120</sub>

Guan-Wu Wang, Koichi Komatsu, Yasujiro Murata & Motoo Shiro

*Nature* **387**, 583–586 (1997)

In this Letter, we overlooked a citation of G. Oszlanyi *et al.*, *Phys. Rev. B* **54**, 11849 (1996), who reported the observation of covalently bound (C<sub>60</sub>)<sub>2</sub><sup>2-</sup> dianions from the X-ray powder diffraction patterns of the metastable phases of KC<sub>60</sub> and RbC<sub>60</sub>. □

### The complete genome sequence of the gastric pathogen *Helicobacter pylori*

Jean-F. Tomb, Owen White, Anthony R. Kerlavage, Rebecca A. Clayton, Granger G. Sutton, Robert D. Fleischmann, Karen A. Ketchum, Hans Peter Klenk, Steven Gill, Brian A. Dougherty, Karen Nelson, John Quackenbush, Lixin Zhou, Ewen F. Kirkness, Scott Peterson, Brendan Loftus, Delwood Richardson, Robert Dodson, Hanif G. Khalak, Anna Glodek, Keith McKenney, Lisa M. Fitzegerald, Norman Lee, Mark D. Adams, Erin K. Hickey, Douglas E. Berg, Jeanine D. Gocayne, Teresa R. Utterback, Jeremy D. Peterson, Jenny M. Kelley, Matthew D. Cotton, Janice M. Weidman, Claire Fujii, Cheryl Bowman, Larry Watthey, Erik Wallin, William S. Hayes, Mark Borodovsky, Peter D. Karp, Hamilton O. Smith, Claire M. Fraser & J. Craig Venter

*Nature* **388**, 539–547 (1997)

In this Article, we incorrectly stated that the amino acids lysine and arginine are twice as abundant in *H. pylori* proteins as they are in those of *Haemophilus influenzae* and *Escherichia coli*. This statement was derived from amino-acid analyses that compared absolute differences in abundance, but these do not reflect the frequencies with which amino acids are found in the organisms in question. The actual abundance of arginine in *H. pylori*, *H. influenzae* and *E. coli* is 3.5, 4.5 and 5.5%, respectively; the abundance of lysine in these organisms is 8.9, 6.3 and 4.4%, respectively. This oversight is particularly unfortunate because Russell H. Doolittle, who wrote an accompanying News and Views on our Article and brought this to our attention, was led to comment on the significance of our inaccurate observation. We regret this and any other misunderstanding that our error may have caused. □

# The complete genome sequence of the gastric pathogen *Helicobacter pylori*

Jean-F. Tomb\*, Owen White\*, Anthony R. Kerlavage\*, Rebecca A. Clayton\*, Granger G. Sutton\*, Robert D. Fleischmann\*, Karen A. Ketchum\*, Hans Peter Klenk\*, Steven Gill\*, Brian A. Dougherty\*, Karen Nelson\*, John Quackenbush\*, Lixin Zhou\*, Ewen F. Kirkness\*, Scott Peterson\*, Brendan Loftus\*, Delwood Richardson\*, Robert Dodson\*, Hanif G. Khalak\*, Anna Glodek\*, Keith McKenney\*, Lisa M. Fitzegerald\*, Norman Lee\*, Mark D. Adams\*, Erin K. Hickey\*, Douglas E. Berg†, Jeanine D. Gocayne\*, Teresa R. Utterback\*, Jeremy D. Peterson\*, Jenny M. Kelley\*, Matthew D. Cotton\*, Janice M. Weidman\*, Claire Fujii\*, Cheryl Bowman\*, Larry Watthey\*, Erik Wallin‡, William S. Hayes§, Mark Borodovsky§, Peter D. Karp||, Hamilton O. Smith‡, Claire M. Fraser\* & J. Craig Venter\*

\* The Institute for Genomic Research, 9712 Medical Center Drive, Rockville, Maryland 20850, USA

† Department of Molecular Biology, School of Medicine, Washington University St Louis, 660 S. Euclid Avenue, St Louis, Missouri 63110, USA

‡ Department of Biochemistry, Arrhenius Laboratory, Stockholm University, S-106 91 Stockholm, Sweden

§ School of Biology, Georgia Tech, Atlanta, Georgia 30332, USA

|| SRI International, Artificial Intelligence Center, 333 Ravenswood Avenue, Menlo Park, California 94025, USA

¶ Department of Molecular Biology and Genetics, School of Medicine, Johns Hopkins University, 725 N. Wolfe Street, Baltimore, Maryland 21205, USA

***Helicobacter pylori*, strain 26695, has a circular genome of 1,667,867 base pairs and 1,590 predicted coding sequences. Sequence analysis indicates that *H. pylori* has well-developed systems for motility, for scavenging iron, and for DNA restriction and modification. Many putative adhesins, lipoproteins and other outer membrane proteins were identified, underscoring the potential complexity of host-pathogen interaction. Based on the large number of sequence-related genes encoding outer membrane proteins and the presence of homopolymeric tracts and dinucleotide repeats in coding sequences, *H. pylori*, like several other mucosal pathogens, probably uses recombination and slipped-strand mispairing within repeats as mechanisms for antigenic variation and adaptive evolution. Consistent with its restricted niche, *H. pylori* has a few regulatory networks, and a limited metabolic repertoire and biosynthetic capacity. Its survival in acid conditions depends, in part, on its ability to establish a positive inside-membrane potential in low pH.**

For most of this century the cause of peptic ulcer disease was thought to be stress-related and the disease to be prevalent in hyperacid producers. The discovery<sup>1</sup> that *Helicobacter pylori* was associated with gastric inflammation and peptic ulcer disease was initially met with scepticism. However, this discovery and subsequent studies on *H. pylori* have revolutionized our view of the gastric environment, the diseases associated with it, and the appropriate treatment regimens<sup>2</sup>.

*Helicobacter pylori* is a micro-aerophilic, Gram-negative, slow-growing, spiral-shaped and flagellated organism. Its most characteristic enzyme is a potent multisubunit urease<sup>3</sup> that is crucial for its survival at acidic pH and for its successful colonization of the gastric environment, a site that few other microbes can colonize<sup>2</sup>. *H. pylori* is probably the most common chronic bacterial infection of humans, present in almost half of the world population<sup>2</sup>. The presence of the bacterium in the gastric mucosa is associated with chronic active gastritis and is implicated in more severe gastric diseases, including chronic atrophic gastritis (a precursor of gastric carcinomas), peptic ulceration and mucosa-associated lymphoid tissue lymphomas<sup>2</sup>. Disease outcome depends on many factors, including bacterial genotype, and host physiology, genotype and dietary habits<sup>4,5</sup>. *H. pylori* infection has also been associated with persistent diarrhoea and increased susceptibility to other infectious diseases<sup>6</sup>.

Because of its importance as a human pathogen, our interest in its biology and evolution, and the value of complete genome sequence information for drug discovery and vaccine development, we have

**Table 1 Genome features**

General	
Coding regions (91.0%)	
Stable RNA (0.7%)	
Non-coding repeats (2.3%)	
Intergenic sequence (6.0%)	
RNA	
Ribosomal RNA	Coordinates
23S-5S	445,306-448,642 bp
23S-5S	1,473,557-1,473,919 bp
16S	1,209,082-1,207,584 bp
16S	1,511,138-1,512,635 bp
5S	448,041-448,618 bp
Transfer RNA	
36 species (7 clusters, 12 single genes)	
Structural RNA	
1 species (ssrD)	629,845-630,124 bp
DNA	
Insertion sequences	
IS605 13 copies (5 full-length, 8 partial)	
IS606 4 copies (2 full-length, 2 partial)	
Distinct G + C regions	
region 1 (33% G + C) 452-479 kb	Associated genes
region 2 (35% G + C) 539-579 kb	IS605, 5SRNA and repeat 7; <i>virB4</i>
region 3 (33% G + C) 1,049-1,071 kb	cag PAI (Fig. 4)
region 4 (43% G + C) 1,264-1,276 kb	IS605, 5SRNA and repeat 7
region 5 (33% G + C) 1,590-1,602 kb	β and β' RNA polymerase, EF-G ( <i>fusA</i> )
	two restriction/modification systems
Coding sequences	
1,590 coding sequences (average 945 bp)	
1,091 identified database match	
499 no database match	

sequenced the genome of a representative *H. pylori* strain by the whole-genome random sequencing method as described for *Haemophilus influenzae*<sup>7</sup>, *Mycoplasma genitalium*<sup>8</sup> and *Methanococcus jannaschii*<sup>9</sup>.

**General features of the genome**

**Genome analysis.** The genome of *H. pylori* strain 26695 consists of a circular chromosome with a size of 1,667,867 base pairs (bp) and average G + C content of 39% (Figs 1 and 2). Five regions within the genome have a significantly different G + C composition (Table 1 and Fig. 1). Two of them contain one or more copies of the insertion sequence IS605 (see below) and are flanked by a 5S ribosomal RNA sequence at one end and a 521 bp repeat (repeat 7) near the other. These two regions are also notable because they contain genes involved in DNA processing and one contains 2 orthologues of the *virB4/ptl* gene, the product of which is required for the transfer of oncogenic T-DNA of *Agrobacterium* and the secretion of the pertussis toxin by *Bordetella pertussis*<sup>10</sup>. Another region is the *cag* pathogenicity island (PAI), which is flanked by 31-bp direct repeats, and appears to be the product of lateral transfer<sup>11</sup>.

**RNA and repeat elements.** Thirty-six tRNA species were identified using tRNAscan-SE<sup>12</sup>. These are organized into 7 clusters plus 12 single genes. Two separate sets of 23S–5S and 16S ribosomal RNA (rRNA) genes were identified, along with one orphan 5S gene and one structural RNA gene (Table 1). Associated with each of the two 23S–5S gene clusters is a 6-kilobase (kb) repeat containing a complete operon of 5 ORFs that have no database matches.

Eight repeat families (>97% identity) varying in length from 0.47 to 3.8 kb were found in the chromosome (Figs 1 and 2). Members of repeat 7 are found in intergenic regions, while the others are associated with coding sequences and may represent gene duplications. Repeats 1, 2, 3 and 6 are associated with genes that encode outer-membrane proteins (OMP) (Fig. 3).

Two distinct insertion sequence (IS) elements are present. There are five full-length copies of the previously described IS605<sup>11,13</sup> and two of a newly discovered element designated IS606. In addition, there are eight partial copies of IS605 and two partial copies of IS606. Both elements encode two divergently transcribed transposases (TnpA and TnpB). IS606 has less than 50% nucleotide identity with IS605 and the IS606 transposases have 29% amino-acid identity with their IS605 counterpart. Both copies of the IS606 TnpB may be non-functional owing to frameshifts.

**Origin of replication.** As a typical eubacterial origin of replication was not identified<sup>14</sup>, we arbitrarily designated basepair one at the start of a 7-mer repeat, (AGTGATT)<sub>26</sub>, that produces translational stops in all reading frames, as this repeated DNA is unlikely to contain any coding sequence.

**Open reading frames.** One thousand five hundred and ninety predicted coding sequences were identified. They were searched against a non-redundant protein database resulting in 1,091 putative identifications that were assigned biological roles using a classification system adapted from Riley<sup>15</sup> (Table 2). The 1,590 predicted genes had an average size of 945 bp, similar to that observed in other prokaryotes<sup>7–9</sup>, and no genome-wide strand bias was observed (Fig. 2). More than 70% of the predicted proteins in *H. pylori* have a calculated isoelectric point (pI) greater than 7.0, compared to ~40% in *H. influenzae* and *E. coli*. The basic amino acids, arginine and lysine, occur twice as frequently in *H. pylori* proteins as in those of *H. influenzae* and *E. coli*, perhaps reflecting an adaptation of *H. pylori* to gastric acidity.

**Paralogous families.** Ninety-five paralogous gene families comprising 266 gene products (16% of the total) were identified (www.tigr.org/tdb/mdb/hpdb/hpdb.html). Of these, 67 (173 proteins) have an assigned role. Sixty-four have only 2 members, while the porin/adhesin-like outer membrane protein family (Fig. 2) is the largest with 32 members. The largest number of paralogues with assigned roles fall into the functional categories of cell

envelope, transport and binding proteins, and proteins involved in replication. The large number of cell envelope proteins might reflect either a reduced biosynthetic capacity or a need to adapt to the challenging gastric environment.

**Cell division and protein secretion**

The gene content of *H. pylori* suggests that the basic mechanisms of replication, cell division and secretion are similar to those of *E. coli* and *H. influenzae*. However, important differences are noted. For example, apparently missing from the *H. pylori* genome are orthologues of DnaC, MinC, and the secretory chaperonin, SecB. In oriC-type primosome formation, the DnaB and DnaC proteins form a B–C complex that delivers the DnaB helicase to the developing primosome complex<sup>16</sup>. The apparent absence of DnaC in *H. pylori* suggests that either a novel mechanism for recruiting DnaB exists or a DnaC orthologue with no detectable sequence similarity is present. Similar arguments can be made for other seemingly missing important functions.

*H. pylori* has a classical set of bacterial chaperones (DnaK, DnaJ, CbpA, GrpE, GroEL, GroES, and HtpG). The transcriptional regulation of *H. pylori* chaperone genes is likely to be different from that in *E. coli*, as it seems not to have the sigma factors that upregulate chaperone synthesis in *E. coli* (heat-shock sigma 32 and stationary-phase sigma S).

In addition to the SecA-dependent secretory pathway, *H. pylori* has two specialized export systems. One is associated with the *cag* pathogenicity island<sup>11</sup> and the other is the flagellar export pathway which is assembled from orthologues of FliH, FliI, FliP, FlhA, FlhB, FliQ, FliR and FliP<sup>17</sup>. Apparently absent from *H. pylori* is a type IV signal peptidase and orthologues of the dsbABC system, which in other species are required for the maturation of pili and pilin-like structures<sup>18</sup> and assembly of surface structures involved in virulence and DNA transformation<sup>19</sup>.

**Recombination, repair and restriction systems**

Systems for homologous recombination and post-replication, mismatch, excision and transcription-coupled repair appear to be present in *H. pylori*. Also present are genes with similarity to DNA glycosylases which have associated AP endonuclease activity. The RecBCD pathway, which mediates homologous recombination and double-strand break repair, and RecT and RecE orthologues, proteins involved in strand exchange during recombination<sup>20</sup>, seem to be absent. The ability of *H. pylori* to perform mismatch repair is suggested by the presence of methyl transferases, mutS and uvrD. However, orthologues of MutH and MutL were not identified. Components of an SOS system also appear to be absent.

Bacteria commonly use restriction and modification systems to degrade foreign DNA. In *H. pylori*, this defence system is well developed with eleven restriction-modification systems identified on the basis of gene order and similarity to endonucleases, methyltransferases, and specificity subunits. Three type I, one type II, and three type IIS systems were identified, as well as four type III systems, including the recently identified epithelial responsive

**Figure 1** Linear representation of the *H. pylori* 26695 chromosome illustrating the location of each predicted protein-coding region, RNA gene, and repeat elements in the genome. Symbols are as follows: ++, Co<sup>2+</sup>, Zn<sup>2+</sup>, Cd<sup>2+</sup>; ?, unknown; A/G/S, D-alanine/glycine/D-serine; B12, B12/ferric siderophores; E, glutamate; Mo, molybdenum; P, proline; P/G, proline/glycine betaine; Q, glutamine; S, serine; a-k, α-ketoglutarate; a/o, arginine/ornithine; aa, amino acids (specificity unknown); aa2, dipeptides; aaX, oligopeptides; fum, fumarate, succinate; glu, glucose/galactose; h, hemin; lac, L-lactate; mal, malate 2-oxoglutarate; nic, nicotinamide mononucleotides; pyr, pyrimidine nucleosides. Numbers associated with tRNA symbols represent the number of tRNAs at a locus. Numbers associated with GES represent the number of membrane-spanning domains according to the Goldman, Engelman and Steitz scale as calculated by TopPred<sup>47</sup>.

endonuclease, *iceA1*, and its associated DNA adenine methyltransferase (M. HypI) genes<sup>21,22</sup>. In addition to the complete systems, seven adenine-specific, and four cytosine-specific methyltransferases, and one of unknown specificity were found. Each of these has an adjacent gene with no database match, suggesting that they may function as part of restriction-modification systems.

**Transcription and translation**

Although analysis of gene content suggests that *H. pylori* has a basic transcriptional and translational machinery similar to that of *E. coli*, interesting differences are observed. For example, no genes for a catalytic activity in tRNA maturation (*rnd*, *rph*, or *rnpB*) were identified and of the three known ribonucleases involved in mRNA degradation, only polyribonucleotide phosphorylase was found. Twenty-one genes coding for 18 of the 20 tRNA synthetases normally required for protein biosynthesis were found.

As in most other completely sequenced bacterial genomes, the gene for glutamyl-tRNA synthetase, *glnS*, is missing, and the existence of a transamidation process is assumed. It is also possible that the product of the second glutamyl-tRNA synthetase gene, *gltX*, present in *H. pylori*, may have acquired the glutamyl-tRNA synthetase function. *H. pylori* provides the first example of a bacterial genome apparently lacking an asparaginyl-tRNA synthetase gene, *asnS*. A transamidation process to form *Asn-tRNAAsn* from *Asp-tRNAAsn* has been reported for the archaeon *Haloferax volcanii*<sup>22</sup> and may also operate in *H. pylori*. Most intriguing, however, is the finding that in *H. pylori* the genes encoding the  $\beta$  and  $\beta'$  subunits of RNA polymerase are fused. In all studied prokaryotes the two genes are contiguous, but separate, and are part of the same transcriptional unit. Whether this gene fusion in *H. pylori* results in a fused protein, or whether the transcriptional or translational product of the fusion is subject to splicing, is currently not known. It is worth noting that an artificial fusion of the *E. coli*

*rpoB* and *rpoC* genes is viable and results in a transcriptional complex, which has the same stoichiometry as the native complex (K. Severinov, personal communication).

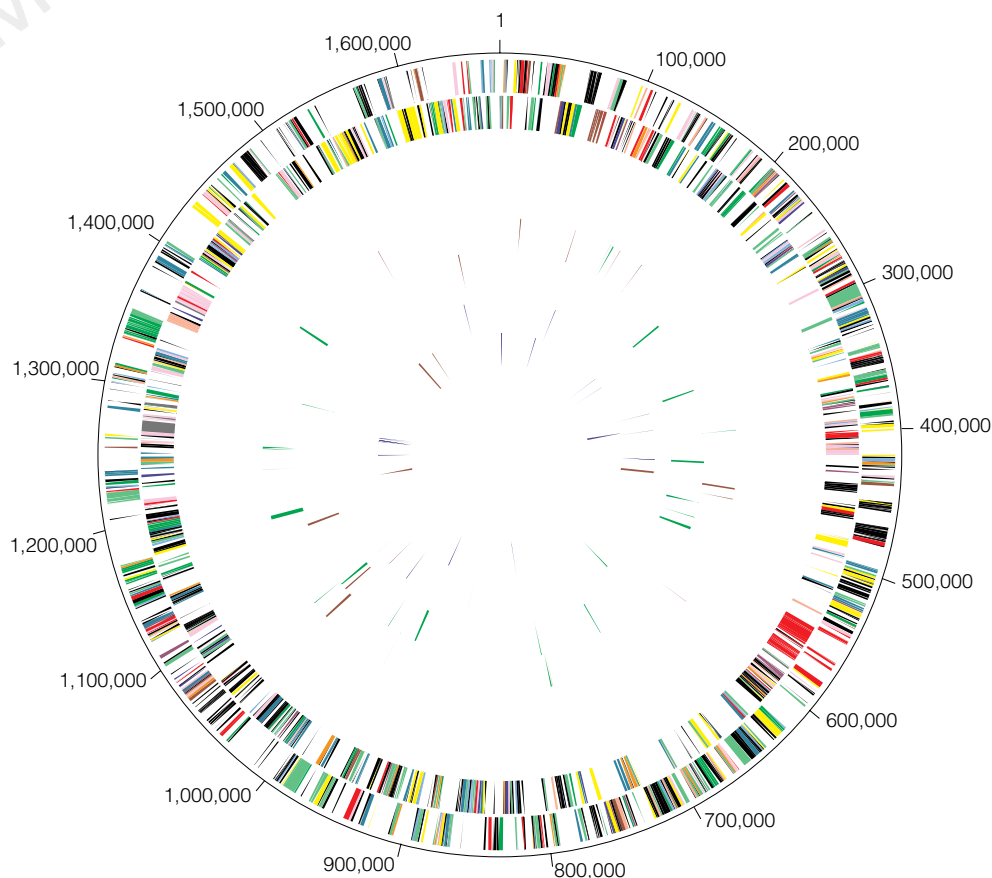
**Adhesion and adaptive antigenic variation**

Most pathogens show tropism to specific tissues or cell types and often use several adherence mechanisms for successful attachment. *H. pylori* may use at least five different adhesins to attach to gastric epithelial cells<sup>5</sup>. One of them, HpaA (HP0797), was previously identified as a lipoprotein in the flagellar sheath and outer membrane<sup>5,23</sup>. In addition to the HpaA orthologue, we have identified 19 other lipoproteins. Few have an identifiable function, but some are likely to contribute to the adherence capacity of the organism.

Two adhesins<sup>24-26</sup>, one of which mediates attachment to the Lewis<sup>b</sup> histo-blood group antigens, belong to the large family of outer membrane proteins (OMP) (Fig. 3) (T. Boren and R. Haas, personal communication). It is conceivable that other members of these closely related proteins also act as adhesins. Given the large number of sequence-related genes encoding putative surface-exposed proteins, the potential exists for recombinational events leading to mosaic organization. This could be the basis for antigenic variation in *H. pylori* and an effective mechanism for host defence evasion, as seen in *M. genitalium*<sup>27</sup>.

At least one other mechanism for antigenic variation could operate in *H. pylori*. The DNA sequence at the beginning of eight genes, including five members of the OMP family, contain stretches of CT or AG dinucleotide repeats (Table 3a). In addition, poly(C) or poly(G) tracts occur within the coding sequence of nine other genes (Table 3b). Slipped-strand mispairing within such repeats are documented features of one mechanism of genotypic variation<sup>28,29</sup>. These mechanisms may have evolved in bacterial pathogens to increase the frequency of phenotypic variation in genes involved in

**Figure 2** Circular representation of the *H. pylori* 26695 chromosome. Outer concentric circle: predicted coding regions on the plus strand classified as to role according to the colour code in Fig. 1 (except for unknowns and hypotheticals, which are in black). Second concentric circle: predicted coding regions on the minus strand. Third and fourth concentric circles: IS elements (red) and other repeats (green) on the plus and minus strand, respectively. Fifth and sixth concentric circles: tRNAs (blue), rRNAs (red), and sRNAs (green) on the plus and minus strand, respectively.



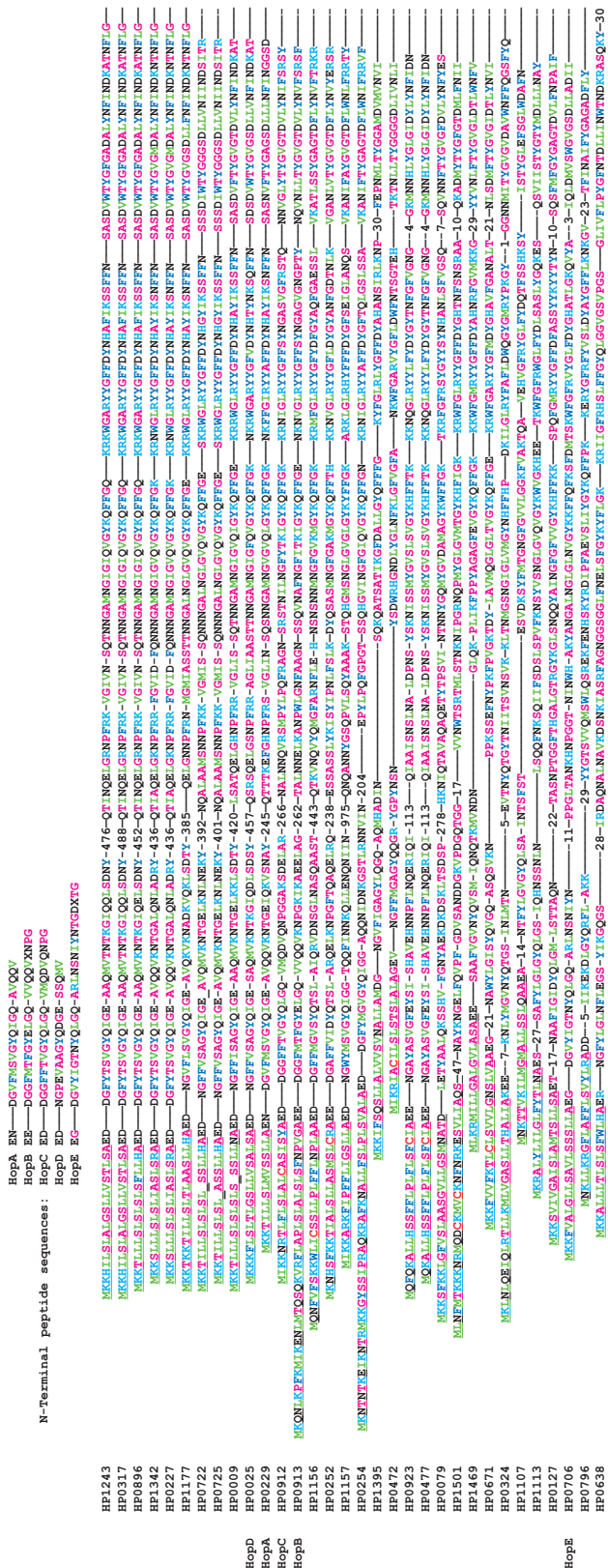


**Figure 3** Multiple sequence alignment of members of the outer membrane protein family of *H. pylori*. These proteins were identified as OMPs based on the characteristic alternating hydrophobic residues at their carboxy termini. All members of this family have one domain of similarity at the amino-terminal end and seven domains of similarity at their carboxy-terminal end. Note that the first 11 of these OMPs share extensive similarity over their entire length. Four of the OMPs were identified as porins (Hops) based on identity to published amino-terminal sequences, represented at the top of the alignment<sup>50</sup>. The most likely

candidate for HopD is HP0913, which has 15 matches to the first 20-residue N-terminal peptide sequence<sup>50</sup>. These differences may be due to strain variability. The program Signal-P<sup>48</sup> was used to identify cleavage sites and signal peptides (underlined). Four of the OMPs have TTG start codons (HP1156, HP0252, HP1113, HP0796). Numbers embedded in the sequences represent amino acids omitted from the alignment. The star symbols indicate that HP722, HP725 and HP9 proteins contain a frameshift in their signal-peptide-coding region. These frameshifts are associated with the presence of dinucleotide repeats (Table 3).

critical interactions with their hosts<sup>28</sup>. Such 'contingency' genes encode surface structures like pilins, lipoproteins or enzymes that produce lipopolysaccharide molecules<sup>28</sup>. Our analysis suggests that the seventeen genes reported in Table 3a,b belong to this category and thus may provide an example of adaptive evolution in *H. pylori*.

Phenotypic variation at the transcriptional level may also operate in *H. pylori*. Examples of repetitive DNA mediating transcriptional control have been documented by the presence of oligonucleotide repeats in promoter regions<sup>29</sup>. Homopolymeric tracts of A or T in potential promoter regions of eighteen genes were found, including eight members of the OMP family (Table 3c).

**Virulence**

The virulence of individual *H. pylori* isolates has been measured by their ability to produce a cytotoxin-associated protein (CagA) and

an active vacuolating cytotoxin (VacA)<sup>5</sup>. The *cagA* gene, though not a virulence determinant, is positioned at one end of a pathogenicity island containing genes that elicit the production of interleukin (IL)-8 by gastric epithelial cells<sup>11,30</sup>. Consistent with its more virulent character, *H. pylori* strain 26695 contains a single contiguous PAI region<sup>11</sup> (Fig. 4).

VacA induces the formation of acidic vacuoles in host epithelial cells, and its presence is associated epidemiologically with tissue damage and disease<sup>31</sup>. VacA may not be the only ulcer-causing factor as 40% of *H. pylori* strains do not produce detectable amounts of the cytotoxin *in vitro*<sup>5</sup>. Sequence differences at the amino terminus and central sections are noted among VacA proteins derived from Tox<sup>+</sup> and Tox<sup>-</sup> strains<sup>31</sup>. This Tox<sup>+</sup> *H. pylori* strain contains the more toxigenic S1a/m1 type cytotoxin and three additional large proteins with moderate similarities to the carboxy-terminal end of the active

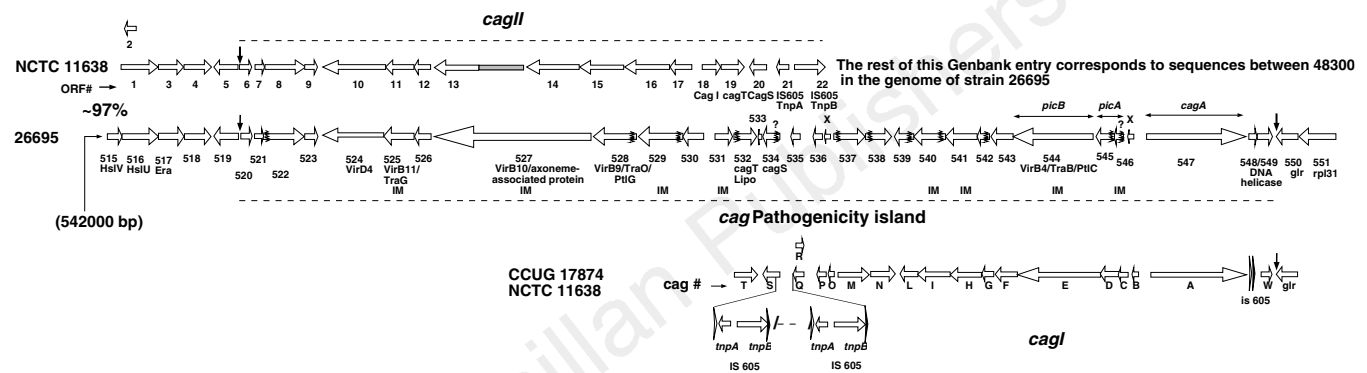


**Figure 4** Comparison between the Cag pathogenicity islands of the sequenced strain, 26695 and the NCTC11638 strain. The twenty nine ORFs of the contiguous PAI in strain 26695 are represented together with the corresponding ORFs from the PAI present in NCTC11638 (AC000108 and U60176). The PAI in NCTC11638 is divided by the IS 605 elements into two regions, *cagl* and *cagII*. The PAI in NCTC11638 is flanked by a 31-bp (TTACAATTTGAGCCCATCTTTAGCTTGTTTT) direct repeat (vertical arrows) as described<sup>11</sup>. Some of the genes encode proteins with similarity to proteins involved either in DNA transfer (Vir and Tra proteins) or in export of a toxin (Ptl protein)<sup>10</sup>. However, these genes do not have the conserved contiguous arrangement found in the VirB, Tra and Ptl operons, suggesting that this PAI is not derived from these systems. Most genes of the PAI have no database match, contrary to a previous suggestion<sup>11</sup>. Thirteen of the proteins have a signal peptide (squiggle line), three of them with a weaker probability (squiggled line+?). The average length of the signal peptides is 25 amino acids, suggesting that this PAI is of Gram-negative origin. Eight proteins are predicted to have at least two membrane-spanning domains and to be integral membrane proteins

(IM)<sup>47</sup>. Although the two PAI are ~97% identical at the nucleotide level, there are several notable and perhaps biologically relevant differences between the two sequences. Four of the genes differ in size. In the PAI of strain 26695, HP 520 and 521 are shorter, whereas HP523 is longer, and HP 527 actually spans both ORF13 and 14. In addition, the N-terminal part of HP527 is 129 amino acids longer than the corresponding region in ORF14. HP548/549 contains a frameshift and is therefore probably inactive in strain 26695. The stippled box preceding ORF13 represents an N-terminal extension not annotated in the Genbank entry for the PAI of NCTC11638. The 'x' indicates ORFs that are neither GeneMark-positive nor GeneSmith-positive, so were not included in our gene list. However, these ORFs may be biologically significant. We do not represent *cagR* as an ORF, because it is completely contained within ORFQ, and is GeneMark-negative.

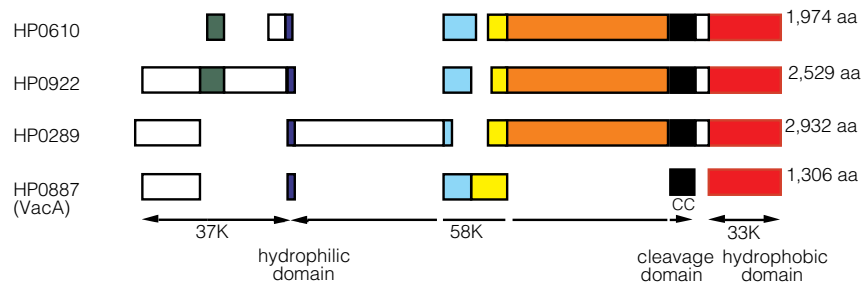


**Figure 5** Conserved domains of VacA and related proteins. HP887 is the vacuolating cytotoxin (*vacA*) gene from *H. pylori* 26695 strain. HP610, HP922 and HP289 are related proteins. Blocks of aligned sequence and the length of each protein are shown. Arrows designate the extents of each VacA domain. The hydrophilic domain (blue boxes) contains the site in VacA at which the N-terminal domain is cleaved into 37K and 58K fragments. The putative cleavage site (ANNNQNS) differs from that of three cytotoxic strains (CCUG 1784, 60190, G39;

AKNDKXES) and is not conserved in the other three VacA-related proteins. The cleavage domain (black boxes) of VacA contains a pair of Cys residues 60 residues upstream from the site at which the C terminus is cleaved. These residues are not conserved in the other three proteins. The 33K C-terminal hydrophobic domain (red boxes) in VacA is thought to form a pore through which the toxin is secreted. The other three proteins show 26-31% sequence similarity to VacA in this region. The other coloured boxes represent regions of similarity.

cytotoxin (~26–31%) (Fig. 5). However, they lack the paired-cysteine residues and the cleavage site required for release of the VacA toxin from the bacterial membrane<sup>31</sup> (Fig. 5). We propose that these proteins may be retained on the outside surface of the cell membrane and contribute to the interaction between *H. pylori* and host cells.

The surface-exposed lipopolysaccharide (LPS) molecule plays an important role in *H. pylori* pathogenesis<sup>32</sup>. The LPS of *H. pylori* is several orders of magnitude less immunogenic than that of enteric bacteria<sup>33</sup> and the O antigen of many *H. pylori* isolates is known to mimic the human Lewis<sup>x</sup> and Lewis<sup>y</sup> blood group antigen<sup>32</sup>. Genes for synthesis of the lipid A molecule, the core region, and the O antigen were identified. Two genes with low similarity to fucosyltransferases (HP379, HP651) were found and may play a role in the LPS-Lewis antigen molecular mimicry. Our analysis also suggests that three genes, two glycosyltransferases (HP208 and HP619) and one fucosyltransferase (HP379), may be subject to phase variation (Table 3a, b).

As with other pathogens, *H. pylori* probably requires an iron-scavenging system for survival in the host<sup>5</sup>. Genome analysis suggests that *H. pylori* has several systems for iron uptake. One is analogous to the siderophore-mediated iron-uptake *fec* system of *E. coli*<sup>34</sup>, except that it lacks the two regulatory proteins (FecR and FecI) and is not organized in a single operon. Unlike other studied systems, *H. pylori* has three copies of each of *fecA*, *exbB* and *exbD*. A second system, consisting of a *feoB*-like gene without *feoA*, suggests that *H. pylori* can assimilate ferrous iron in a fashion similar to the anaerobic *feo* system of *E. coli*. Other systems for iron uptake present in *H. pylori* consist of the three *frpB* genes which encode proteins similar to either haem- or lactoferrin-binding proteins. Finally, *H. pylori* contains NapA, a bacterioferritin<sup>34</sup>, and Pfr, a non-haem cytoplasmic iron-containing ferritin used for storage of iron<sup>35</sup>. The global ferric uptake regulator (Fur) characterized in other bacteria is also present in *H. pylori*. Consensus

sequences for Fur-binding boxes were found upstream of two *fecA* genes, the three *frnB* genes and *fur*.

*H. pylori* motility is essential for colonization<sup>36</sup>. It enables the bacterium to spread into the viscous mucous layer covering the gastric epithelium. At least forty proteins in the *H. pylori* genome appear to be involved in the regulation, secretion and assembly of the flagellar architecture. As has been reported for the *flaA* and *flaB* genes, we identified sigma 28 and sigma 54-like promoter elements upstream of many flagellar genes, underscoring the complexity of the transcriptional regulation of the flagellar regulon<sup>5</sup>.

**Acidity, pH and acid tolerance**

*H. pylori* is unusual among pathogenic bacteria in its ability to colonize host cells in an environment of high acidity. As it enters the gastric environment by oral ingestion, the organism is transiently subjected to the extreme pH of the lumen side of the gastric mucous layer (pH ~2). The survival of *H. pylori* in acidic environments is probably due to its ability to establish a positive inside-membrane potential<sup>37</sup> and subsequently to modify its microenvironment through the action of urease and the release of factors that inhibit acid production by parietal cells<sup>5</sup>. A switch in membrane polarity provides an electrical barrier that prevents the entry of protons (H<sup>+</sup>). A positive cell interior can be created by the active extrusion of anions or by a proton diffusion potential. The latter model appears more likely as no clear mechanism for electrogenic anion efflux is apparent in the genome. A proton diffusion potential would require the anion permeability of the cytoplasmic membrane to be low and, thus far, only three anion transporters have been identified. However, it remains to be determined whether anion conductances are associated with other proteins: the MDR-like transporters (HP600, HP1082 and HP1206) or hypotheticals. Although it has been suggested that proton-translocating P-type ATPases could mediate survival in acid conditions by the extrusion of protons from the cytoplasm<sup>38</sup>, this idea is not supported by the identified transporter

**Table 3 Homopolymeric tracts and dinucleotide repeats in *H. pylori***

HP no.	ID	No. of repeats	Gene status	Poly(A) or Poly(T) tracts in 5' intergenic region
9	OMP	11 CT	Off	Poly(A)
208	glycos. transf.	11 AG	Truncated	Poly(A)
638	OMP	6 CT	On	No
722	OMP	8 CT	Off	Poly(T)
725	OMP	6 CT	Off	Poly(T)
744	Hypo	9 AG	Truncated	No
896	OMP	11 CT	On	Poly(A)
1417	Cons. Hypo	9 AG	Truncated	No

Nucleotide sequence at the beginning of HP0722 showing the CT dinucleotide repeat and the poly T tract. The putative ribosome binding site is shown in green. Translation starting at the designated methionine leads to a truncated product. The addition or deletion of two CT repeats, by 'slipped-strand mispairing', will restore the frame.

CCAAAAATCTTTTTTTTTTTTTTTTGAATCCAATAAATTTATGGTAAAGT-37bp-TTACAATAAAAAAATTACTTTAAGGAACATTT  
**TATG**AAAAAGACAATCTACTCTCTCTCTCTCTCTCGCTTCATCGCTTGGCACGCTGAAGACAACGGCTTTTTTGTGAGCGCCGGCT  
 Y E K D N S T L S L S L A S S L L H A E D N G F V S A G Y  
**M** K K T I L L S L S L S L H R S C T L K T T A F L \*

(b) Homopolymeric poly(C) and poly(G) tracts within coding sequence

HP no.	ID	Tract length	Gene status
58	Hypo	C15	Off
217	Hypo	G12	On
379	fucosyl transf.	C13	On
464	Type1 R	C15	On
619	glycos. transf.	C13	Truncated
651	Hypo	C13	On
1353	Hypo	C15	Truncated
1471	Type1S-R	G14	On
1522	Methyl ase	G12	Truncated

Genes possibly regulated by homopolymeric poly(A) or poly(T) tracts in 5' intergenic regions

HP no.	ID	Tract	HP no.	ID	Tract	HP no.	ID	Tract
9	OMP	A14	25	OMP	T15	208	<i>rfaJ</i>	A11
227	OMP	T14	228	IMP	A14	349	<i>pyrG</i>	T15
350	IMP	A15	547	<i>cagA</i>	A14	629	Hypo	T15
722	OMP	T16	725	OMP	T14	733	Hypo	T13
876	<i>frpB</i>	T16	896	OMP	A14	912	OMP	T13
1342	OMP	A14	1400	<i>fecA</i>	A16			

genes. The P-type ATPase sequences in *H. pylori* (*copAB*, HP791, and HP1503) are more closely related to divalent cation transporters than to ATPases with specificity for protons or monovalent cations. One of them, HP0791, is involved in Ni<sup>2+</sup> supply, an essential component of urease activity<sup>39</sup>. The others may be involved in the elimination of toxic metals from the cytoplasm and not in pH regulation.

Additional mechanisms of pH homeostasis may well contribute to *H. pylori* survival. A change in protein content observed in response to a shift of extracellular pH from 7.5 to 3.0 suggests the presence of an acid-inducible response<sup>40</sup>. Although *H. pylori* lacks most orthologues of the genes that are acid-induced in *E. coli* and *Salmonella typhimurium*, including the amino-acid decarboxylases and formate hydrogen lyase, certain virulence factors, outer membrane

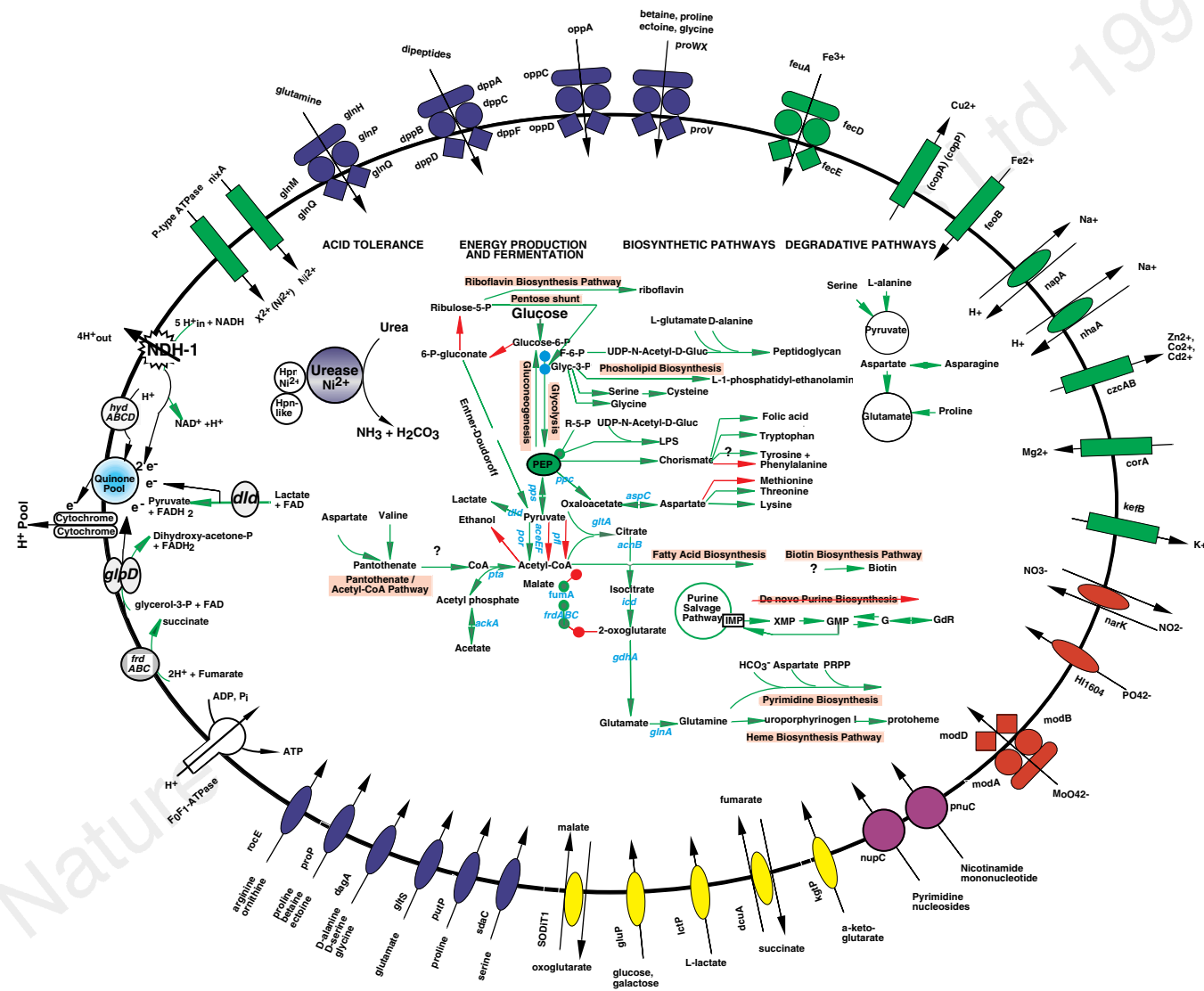


**Figure 6** Solute transport and metabolic pathways of *Helicobacter pylori*. Transporters identified by sequence comparisons are characteristic of Gram-negative bacteria. Colours correspond to transport role categories defined by Riley<sup>15</sup>: blue, amino acids, peptides and amines; red, anions; yellow, carbohydrates, organic alcohols and acids; green, cations; and purple, nucleosides, purines and pyrimidines. Numerous permeases (ovals) with specificity for amino acids (*recE*, *proP*, *dagA*, *gltS*, *putP* and *sdaC*) or carbohydrates (*SODiTI*, *gluP*, *lactP*, *cdvA*, *kgtP*) import organic nutrients. Structurally related permease proteins maintain ionic homeostasis by transporting HPO<sub>4</sub><sup>2-</sup> (*HI1604*), NO<sub>3</sub><sup>-</sup> (*narK*), and Na<sup>+</sup> (*nhA*, *napA*). Primary active-transport systems, independent of the proton cycle, are also apparent. Included in this group are ATP-binding protein-cassette (ABC) transporters (composite figures of 2 diamonds, 2 circles, 1 oval) for the uptake of oligopeptides (*oppACD*), dipeptides (*dppABCD*), proline (*proVWX*), glutamine (*glnHMPQ*), molybdenum (*modABD*), and iron III (*fecED*), P-type ATPases that extrude toxic metals from the cell (*copAP* and *cadA*), and the glutathione-regulated potassium-efflux protein (*kefB*). Transporters for the accumulation of ionic cofactors are encoded by *nixA* (Ni<sup>2+</sup> for urease activation), *corA* (Mg<sup>2+</sup> for phosphohydrolases, phosphotransferases, ATPases) and *feoB* (Fe<sup>2+</sup>

import under anaerobic conditions for cytochromes, catalase). An integrated view of the main components of the central metabolism of *H. pylori* strain 26695 is presented. The use of glucose as the sole carbohydrate source is emphasized. Urease, a multisubunit Ni<sup>2+</sup>-binding enzyme, is crucial for colonization and for survival of *H. pylori* at acid pH, and is indicated as a complex (purple circle) with Hpn, a Ni<sup>2+</sup>-binding cofactor, and a newly identified Hpn-like protein (HP1432). A question mark is attached to pathways that could not be completely elucidated. Pathways or steps for which no enzymes were identified are represented by a red arrow. Pathways for macromolecular biosynthesis (RNA, DNA and fatty acids) have been omitted. *ackA*, acetate kinase; *acnB*, aconitase B; *aspC*, aspartate aminotransferase; *dld*, D-lactate dehydrogenase; *gdhA*, glutamate dehydrogenase; *glnA*, glutamine synthetase; *gltA*, citrate synthase; *HydABC*, hydrogenase complex; *icd*, isocitrate dehydrogenase; *pfl*, pyruvate formate lyase; *por*, pyruvate ferredoxin oxidoreductase; *ppc*, phosphoenolpyruvate carboxylase; *pps*, phosphoenolpyruvate synthase; *pta*, phosphate acetyltransferase; *gldD*, glycerol-3-phosphate dehydrogenase; NDH-1, NADH-ubiquinone oxidoreductase complex.



proteins, sensor-regulator pairs and other proteins may be acid-induced.

## Regulation of gene expression

Bacteria regulate the transcription of their genes in response to many environmental stimuli, such as nutrient availability, cell density, pH, contact with target tissue, DNA-damaging agents, temperature and osmolarity. In the case of pathogens, the regulated expression of certain key genes is essential for successful evasion of host responses and colonization, adaptation to different body sites, and survival as the pathogen passes to new hosts. In *H. pylori*, global regulatory proteins are less abundant than in *E. coli*. For example, orthologues of many DNA-binding proteins that regulate the expression of certain operons such as OxyR (oxidative stress), Crp (carbon utilization), RpoH (heat shock), and Fnr (fumarate and nitrate regulation) are absent. Only four *H. pylori* proteins have a perfect match to helix–turn–helix (HTH) motifs, a signature of transcription factors; a putative heat-shock protein (HspR), two proteins with no database match (HP1124 and HP1349) and SecA, a component of the general secretory machinery. In contrast, 34 proteins containing an HTH motif were found in *H. influenzae* and 148 in *E. coli*. We identified several other putative regulatory functions, including SpoT and CstA for ‘stringent response’ to amino-acid starvation and to carbon starvation, respectively.

Environmental response requires sensing changes and transmission of this information to cellular regulatory networks. Two-component regulator systems, consisting of a membrane histidine kinase sensor protein and a cytoplasmic DNA-binding response regulator, provide a well studied mechanism for such signal transduction. Four sensor proteins and seven response regulators were found in *H. pylori*, similar to the number found in *H. influenzae*<sup>7</sup>. This is approximately one third the number found in *E. coli* which, in contrast to *H. pylori* and *H. influenzae*, may be exposed to more environments.

## Metabolism

Metabolic pathway analysis of the *H. pylori* genome suggests the following features. *H. pylori* uses glucose as the only source of carbohydrate and the main source for substrate-level phosphorylation. It also derives energy from the degradation of serine, alanine, aspartate and proline. The glycolysis–gluconeogenesis metabolic axis constitutes the backbone of energy production and the start point of many biosynthetic pathways. The biosynthesis of peptidoglycan, phospholipids, aromatic amino acids, fatty acids and cofactors is derived from acetyl-CoA or from intermediates in the glycolytic pathway (Fig. 6). The metabolism of pyruvate reflects the microaerophilic character of this organism. Neither the aerobic pyruvate dehydrogenase (*aceEF*) nor the strictly anaerobic pyruvate formate lyase (*pfl*) associated with mixed-acid fermentation are present. The conversion of pyruvate to acetyl CoA is performed by the pyruvate ferredoxin oxidoreductase (POR), a four-subunit enzyme thus far only described in hyperthermophilic organisms<sup>41</sup>. The tricarboxylic acid cycle (TCA) is incomplete and the glyoxylate shunt is absent. The analysis of degradative pathways, uptake systems and biosynthetic pathways for pyrimidine, purine and haem suggests that *H. pylori* uses several substrates as nitrogen source, including urea, ammonia, alanine, serine and glutamine. The assimilation of ammonia, an abundant product of urease activity, is achieved by the glutamine synthase enzyme and  $\alpha$ -ketoglutarate is transformed into glutamate by glutamate dehydrogenase rather than by the glutamate synthase enzyme.

In *H. pylori*, proton translocation is mediated by the NDH-1 dehydrogenase and the different cytochromes, including the primitive-type cytochrome *cbb3* (Table 2). Four respiratory electron-generating dehydrogenases have been identified, glycerol-3-phosphate dehydrogenase (GlpD), D-lactate dehydrogenase, NADH–ubiquinone oxidoreductase complex (NDH-1), and a hydrogenase complex (HydABC). Our analysis also suggests that

*H. pylori* is not able to use nitrate, nitrite, dimethylsulphoxide, trimethylamine *N*-oxide or thiosulphate as electron acceptors. Much of our metabolic analysis is supported by experimental evidence<sup>41,42</sup>.

## Evolutionary relationships of *H. pylori*

*H. pylori* is currently classified in the Proteobacteria, a large, diverse division of Gram-negative bacteria which includes two other completely sequenced species, *H. influenzae* and *E. coli*. Given this taxonomic placement, based primarily on 16S rRNA sequence comparisons, one might expect the proteins of *H. pylori* more closely to resemble their *H. influenzae* and *E. coli* homologues rather than those in other genomes such as *Synechocystis* sp., *M. genitalium*, *M. pneumoniae*, *M. jannaschii*, and *Saccharomyces cerevisiae*. This is indeed the case for many proteins. There are, however, many examples of *H. pylori* proteins in amino-acid biosynthesis, energy metabolism, translation and cellular processes that have greater sequence similarity to those found in non-Proteobacteria. For example, Dhs1, the initial enzyme in the chorismate biosynthesis pathway is 75.5% similar to *Arabidopsis thaliana* chloroplast Dhs1 gene product, and has minimal sequence similarity to the equivalent *E. coli* AroH, AroF or AroG gene products. The remaining enzymes in this pathway have strong sequence similarity to their *E. coli* counterpart. Similarly, the *H. pylori* prephenate dehydrogenase (TyrA), which converts chorismate to tyrosine, and six out of 15 enzymes in the aspartate amino acid biosynthetic pathways, resemble those from *B. subtilis*. A similar pattern can be seen in a different functional category. Nearly all *H. pylori* tRNA synthetases have eubacterial homologues, mostly with best matches to Proteobacteria species. However, histidyl-tRNA synthetase shows several amino-acid sequence signatures in common with eukaryotic and archaeal (*M. jannaschii*) homologues.

Such observations of discordant sequence similarity are often interpreted as evidence of lateral gene transfer in the evolutionary history of an organism. It is also possible that *H. pylori* diverged early from the lineage that led to the gamma Proteobacteria, and retained more ancient forms of enzymes that have been subsequently replaced or have diverged extensively in *H. influenzae* and *E. coli*.

## Conclusion

Our whole-genome analysis of *H. pylori* gives new insight into its pathogenesis, acid tolerance, antigenic variation and microaerophilic character. The availability of the complete genome sequence will allow further assessment of *H. pylori* genetic diversity. This is an important aspect of *H. pylori* epidemiology as allelic polymorphism within several loci has already been associated with disease outcome<sup>5,21,31</sup>. The extent of molecular mimicry between *H. pylori* and its human host, an underappreciated topic, can now be fully explored<sup>43</sup>. The identification of many new putative virulence determinants should allow critical tests of their roles and thus new insight into mechanisms of initial colonization, persistence of this bacterium during long-term carriage, and the mechanisms by which it promotes various gastroduodenal diseases.

## Methods

*H. pylori* strain 26695 (ref. 44) was originally isolated from a patient in the United Kingdom with gastritis (K. Eaton, personal communication) and was chosen because it colonizes piglets and elicits immune and inflammatory responses. It is also toxigenic, and transformable, and thus amenable to mutational tests of gene function.

The *H. pylori* genome sequence was obtained by a whole-genome random sequencing method previously applied to genomes of *Haemophilus influenzae*<sup>7</sup>, *Mycoplasma genitalium*<sup>8</sup>, and *Methanococcus jannaschii*<sup>9</sup>. Ninety-two per cent of the genome was covered by at least one  $\lambda$  clone and only 0.56% of the genome had single-fold coverage.

Open reading frames (ORFs) and predicted coding regions were identified using three methods. The predicted protein-coding regions were initially defined by searching for ORFs longer than 80 codons. Coding potential analysis of the entire genome was performed with a version of GeneMark<sup>45</sup> trained with a set of *H. pylori* ORFs longer than 600 nucleotides. Coding sequences and potential starts of translation were also determined using GeneSmith (H.S., unpublished), a program that evaluates ORF length, separation of ORFs and overlap and quality of ribosome binding site. ORFs with low GeneMark coding potential, no database match, and not retained by GeneSmith were eliminated. GeneSmith identified 25 ORFs that are smaller than 100 codons, had no database match and were GeneMark negative. Frameshifts were detected by inspecting pairwise alignments, families of orthologues (similar proteins derived from different species) and paralogues (similar proteins from within the same organism), and regions containing homopolymer stretches and dinucleotide repeats. Ambiguities were resolved by an alternative sequencing chemistry (terminator reactions), and by sequencing PCR products obtained using the genomic DNA as template. Frameshifts that remain in the genome are considered authentic and not sequencing artefacts.

To determine their identity, ORFs were searched against a non-redundant amino-acid database as previously described<sup>9</sup>. ORFs were also analysed using 175 hidden Markov models constructed for a number of conserved protein families (pfam v1.0) using hmmer<sup>43</sup>. In addition, all ORFs were searched against the prosite motif database using MacPattern<sup>46</sup>. Families of paralogues were constructed by pairwise searches of proteins using FASTA. Matches that spanned at least 60% of the smaller of the protein pair were retained and visually inspected.

A unix version of the program TopPred<sup>47</sup> was used to identify membrane-spanning domains (MSD) in proteins. Six hundred and sixty three proteins containing at least one MSD were found; of these, 300 had 2 potential MSDs or more. The presence of signal peptides and the probable position of the cleavage site in secreted proteins were detected using Signal-P, a neural net program that had been trained on a curated set of secreted proteins from Gram-negative bacteria<sup>48</sup>. 367 proteins were predicted to have a signal peptide. Lipoproteins were identified by scanning for the presence of a lipobox in the first 30 amino acids of every protein; 20 lipoproteins were identified, eighteen of which were Signal-P positive. Outer-membrane proteins were found by searching for aromatic amino acids at the end of the proteins.

Homopolymer and dinucleotide repeats were found by using RepScan (H.O.S., unpublished) which finds direct repeats of any length. All features identified using these programs were validated by visual inspection to remove false positives. Metabolic pathways were curated by hand and by reference to EcoCyc<sup>49</sup>.

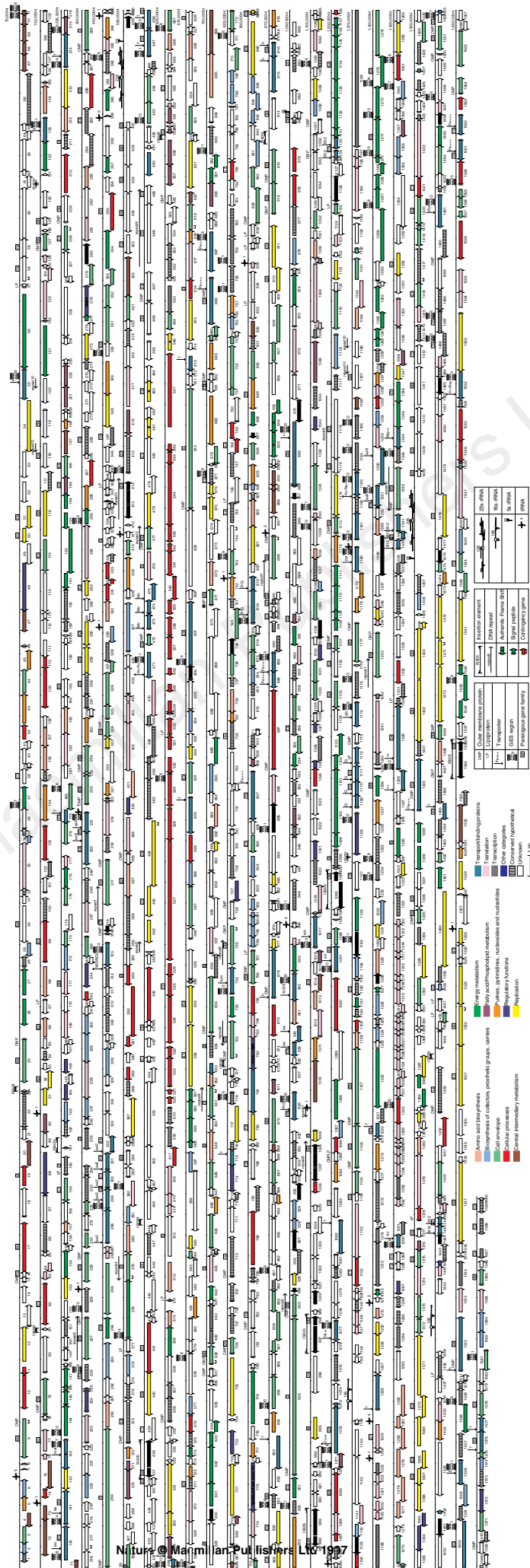
Received 16 May; accepted 1 July 1997.

1. Warren, J. R. & Marshall, B. Unidentified curved bacilli on gastric epithelium in active chronic gastritis. *Lancet* **1**, 1273–1275 (1983).
2. Cover, T. L. & Blaser, M. J. *Helicobacter pylori* infection, a paradigm for chronic mucosal inflammation: pathogenesis and implications for eradication and prevention. *Adv. Int. Med.* **41**, 85–117 (1996).
3. Mobley, H. L. T., Island, M. D. & Hausinger, R. P. Molecular Biology of Microbial Ureasases. *Microbiol. Rev.* **59**, 451–480 (1995).
4. Go, M. F. & Graham, D. Y. How does *Helicobacter pylori* cause duodenal ulcer disease: The bug, the host, or both? *J. Gastroenterol. Hepatol.* (suppl.) **9**, 8–12 (1994).
5. Labigne, A. & de Reuse, H. Determinants of *Helicobacter pylori* pathogenicity. *Infect. Agents Disease* **5**, 191–202 (1996).
6. Clemens, J. et al. Impact of infection by *Helicobacter pylori* on the risk and severity of endemic cholera. *J. Inf. Dis.* **171**, 1653–1656 (1995).
7. Fleischmann, R. D. et al. Whole-genome random sequencing and assembly of *Haemophilus influenzae* Rd. *Science* **269**, 496–512 (1995).
8. Fraser, C. M. et al. The *Mycoplasma genitalium* genome sequence reveals a minimal gene complement. *Science* **270**, 397–403 (1995).
9. Bult, C. J. et al. Complete genome sequence of the methanogenic archaeon, *Methanococcus jannaschii*. *Science* **273**, 1058–1073 (1996).
10. Winans, S. C., Burns, D. L. & Christie, P. J. Adaptation of a conjugal transfer system for the export of pathogenic macromolecules. *Trends Microbiol.* **4**, 64–68 (1996).
11. Censini, S. et al. Cag, a pathogenicity island of *Helicobacter pylori*, encodes type-I-specific and disease-associated virulence factors. *Proc. Natl Acad. Sci. USA* **93**, 14648–14653 (1996).
12. <http://genome.wustl.edu/eddy/low/trnAscAn-SE-Manual/Manual.html>
13. Akopyants, N. S., Kersulyte, D. & Berg, D. E. DNA rearrangement in the 40 kb cag (virulence) region in the *Helicobacter pylori* genome. *Gut* **39** (suppl. 2), A67 (1996).
14. Marczynski, G. T. & Shapiro, L. Bacterial chromosome origins of replication. *Curr. Opin. Gen. Dev.* **3**, 775–782 (1993).
15. Riley, M. Functions of gene products of *Escherichia coli*. *Microbiol. Rev.* **57**, 862–952 (1993).
16. Kornberg, A. & Baker, T. A. Replication mechanisms and operations in DNA replication. (ed. Kornberg, A. & Baker, T.) 471–510 (Freeman, New York, 1992).

17. Macnab, R. M. in *Escherichia coli and Salmonella Cellular and Molecular Biology* (eds Neidhardt, F. C. et al.) 123–145 (ASM, Washington DC, 1996).
18. Strom, M. S., Nunn, D. N. & Lory, S. Posttranslational processing of type IV prepilin and homologs by PilD of *Pseudomonas aeruginosa*. *Meth. Enzymol.* **235**, 527–540 (1994).
19. Bardwell, J. C. Building bridges: disulphide bond formation in the cell. *Mol. Microbiol.* **14**, 199–205 (1994).
20. Linn, S. in *Escherichia coli and Salmonella Cellular and Molecular Biology* (eds Neidhardt, F. C. et al.) 764–772 (ASM, Washington D.C., 1996).
21. Peek, R. M., Thompson, S. A., Atherton, J. C., Blaser, M. J. & Miller, G. G. Expression of iceA, a novel ulcer-associated *Helicobacter pylori* gene, is induced by contact with gastric epithelial cells and is associated with enhanced mucosal IL-8. *Gut* **39** (suppl. 2), A71 (1996).
22. Curnow, A. W., Ibba, M. & Soll, D. tRNA-dependent asparagine formation. *Nature* **382**, 589–590 (1996).
23. Jones, A. C., Foynes, S., Cockayne, A. & Penn, C. W. Gene cloning of a flagellar sheath protein of *Helicobacter pylori* shows its identity with the putative adhesin, HpaA. *Gut* **39** (suppl. 2), A62 (1996).
24. Boren, T., Falk, P., Roth, K. A., Larson, G. & Normark, S. Attachment of *Helicobacter pylori* to human gastric epithelium mediated by blood group antigens. *Science* **262**, 1892–1895 (1993).
25. Iver, D. et al. The *Helicobacter pylori* blood group antigen binding adhesin. *Gut* **39** (suppl. 2), A55 (1996).
26. Odenbreit, S., Till, M. & Haas, R. Optimized blaM-transposon shuttle mutagenesis of *Helicobacter pylori* allows identification of novel genetic loci involved in bacterial virulence. *Mol. Microbiol.* **20**, 361–373 (1996).
27. Peterson, S. N. et al. Characterization of repetitive DNA in the *Mycoplasma genitalium* genome: possible role in the generation of antigenic variation. *Proc. Natl Acad. Sci. USA* **92**, 11829–11833 (1995).
28. Moxon, E. R., Rainey, P. B., Nowak, M. A. & Lenski, R. E. Adaptive evolution of highly mutable loci in pathogenic bacteria. *Curr. Biol.* **4**, 24–33 (1994).
29. Jonsson, A. B., Nyberg, G. & Normark, S. Phase variation of gonococcal pili by frameshift mutation in pilC, a novel gene for pilus assembly. *EMBO J.* **10**, 477–488 (1991).
30. Tumuru, M. K. R., Sharma, S. A. & Blaser, M. J. *Helicobacter pylori* picB, a homologue of the *Bordetella pertussis* toxin secretion protein, is required for induction of IL-8 in gastric epithelial cells. *Mol. Microbiol.* **18**, 867–876 (1995).
31. Atherton, J. C. et al. Mosaicism in vacuolating cytotoxin alleles of *Helicobacter pylori*. Association of specific vacA types with cytotoxin production and peptic ulceration. *J. Biol. Chem.* **270**, 17771–17777 (1995).
32. Moran, A. P. The role of lipopolysaccharide in *Helicobacter pylori* pathogenesis. *Aliment. Pharmacol. Ther.* **10** (suppl. 1), 39–50 (1996).
33. Baker, P. J. et al. Molecular structures that influence the immunomodulatory properties of the lipid A and inner core region oligosaccharides of bacterial lipopolysaccharides. *Infect. Immun.* **62**, 2257–2269 (1994).
34. Earhart, C. F. in *Escherichia coli and Salmonella Cellular and Molecular Biology* (eds Neidhardt, F. C. et al.) 1075–1090 (ASM, Washington DC, 1996).
35. Evans, D. J. Jr, Evans, D. G., Lampert, H. C. & Nakano, H. Identification of four new prokaryotic bacterioferritins, from *Helicobacter pylori*, *Anabaena variabilis*, *Bacillus subtilis* and *Treponema pallidum*, by analysis of gene sequences. *Gene* **153**, 123–127 (1995); Frazier, B. A. et al. Paracrystalline inclusions of a novel ferritin containing nonheme iron, produced by the human gastric pathogen *Helicobacter pylori*: evidence for a third class of ferritins. *J. Bacteriol.* **175**, 966–972 (1993).
36. Suerbaum, S. The complex flagella of gastric *Helicobacter* species. *Trends Microbiol.* **3**, 168–170 (1995).
37. Martin, A., Zychlinsky, E., Keyhan, M. & Sachs, G. Capacity of *Helicobacter pylori* to generate ionic gradients at low pH is similar to that of bacteria which grow under strongly acidic conditions. *Infect. Immun.* **64**, 1434–1436 (1996).
38. Melchers, K. et al. Cloning and membrane topology of a P type ATPase from *Helicobacter pylori*. *J. Biol. Chem.* **271**, 446–457 (1996).
39. Melchers, K. et al. Cloning and analysis of two P type ion pumps of *Helicobacter pylori*, a cation resistance ATPase and a membrane pump necessary for urease activity. *Gut* **39** (suppl. 2), A67 (1996).
40. McGowan, C. C., Cover, T. L. & Blaser, M. J. *Helicobacter pylori* and gastric acid: biological and therapeutic implications. *Gastroenterology* **110**, 926–938 (1996).
41. Hughes, N. J., Chalk, T. L., Clayton, C. L. & Kelly, D. J. Identification of carboxylation enzymes and characterization of a novel four-subunit pyruvate:flavodoxin oxidoreductase from *Helicobacter pylori*. *J. Bacteriol.* **177**, 3953–3959 (1995).
42. Mendz, G. L. & Hazell, S. L. Amino acid utilization by *Helicobacter pylori*. *Int. J. Biochem. Cell. Biol.* **27**, 1085–1093 (1995).
43. Sonhammer, E. L. L., Eddy, S. R. & Durbin, R. Pfam: A comprehensive database of protein families based on seed alignments. *Proteins* (in the press).
44. Akopyants, N. S., Eaton, K. A. & Berg, D. E. Adaptive mutation and co-colonization during *Helicobacter pylori* infection of gnotobiotic piglets. *Infect. Immun.* **63**, 116–121 (1995).
45. Borodovsky, M., Rudd, K. E. & Koonin, E. V. Intrinsic and extrinsic approaches for detecting genes in a bacterial genome. *Nucleic Acids Res.* **22**, 4756–4767 (1994).
46. Fuchs, R. MacPattern: protein pattern searching on the Apple Macintosh. *Comput. Appl. Biosci.* **7**, 105–106 (1991).
47. Claros, M. G. & von Heijne, G. TopPred II: an improved software for membrane protein structure predictions. *Comput. Appl. Biosci.* **10**, 685–686 (1994).
48. Nielsen, H., Engelbrecht, J., Brunak, S. & von Heijne, G. Identification of prokaryotic and eukaryotic signal peptides and prediction of their cleavage sites. *Protein Eng.* **10**, 1–6 (1997).
49. Karp, P. D., Riley, M., Paley, S. M., Pellegrini-Toole, A. & Krummenacker, M. EcoCyc: Encyclopedia of *Escherichia coli* genes and metabolism. *Nucleic Acids Res.* **25**, 43–51 (1997).
50. Doig, P., Exner, M. M., Hancock, R. E. & Trust, T. J. Isolation and characterization of a conserved porin protein from *Helicobacter pylori*. *J. Bacteriol.* **177**, 5447–5452 (1995).

**Acknowledgements.** D.E.B., M.B. and W.H. are supported by grants from the NIH; P.K. is supported by a grant from the National Center for Research Resources. We thank N. S. Akopyants for preparing high quality chromosomal DNA from *H. pylori* strain 26695; M. Heaney, J. Scott, A. Saeed and R. Shirley for software and database support; and V. Sapiro, B. Vincent, J. Meehan and D. Mass for computer system support.

Correspondence and requests for materials should be addressed to J.-F.T. (e-mail: ghp@tigr.org). The annotated genome sequence and gene family alignments are available on the World-Wide Web site at <http://www.tigr.org/tdb/mdb/hpdb/hpdb.html>. The sequence has been deposited with GenBank under accession number AE000511.





HP0332	cell division topological specificity factor (mifE)	33.8%	HP1270	subunit (NQO10)	-1.0%	HP1101	(devB) glucose-6-phosphate dehydrogenase (g6pD)	29.2%
HP0979	cell division protein (ftsZ)	43.3%	HP1271	NADH-ubiquinone oxidoreductase, NQO11 subunit (NQO11) (Paracoccus denitrificans)	42.6%	HP1495	transaldolase (tal)	36.7%
HP1159	cell filamentation protein (fic)	63.2%	HP1272	NADH-ubiquinone oxidoreductase, NQO12 subunit (NQO12)	43.2%	HP1088	transketolase A (tktA)	33.5%
<b>Cell killing</b>						HP0354	transketolase B (tktB)	46.7%
HP0887	vacuolating cytotoxin	94.7%						39.7%
<b>Chaperones</b>								
HP0010	chaperone and heat shock protein (groEL)	99.6%	HP1273	NADH-ubiquinone oxidoreductase, NQO14 subunit (NQO14)	40.2%	<i>Sugars</i>		
HP0109	chaperone and heat shock protein 70 (dnaK)	63.4%	HP1266	NADH-ubiquinone oxidoreductase, NQO3 subunit (NQO3)	31.2%	HP0574	galactosidase acetyltransferase (lacA)	41.0%
HP0210	chaperone and heat shock protein C62.5 (htpG)	46.5%	HP1263	NADH-ubiquinone oxidoreductase, NQO4 subunit (NQO4) (Triticum aestivum)	31.6%	HP0360	UDP-glucose 4-epimerase	43.1%
HP0011	co-chaperone (groES)	99.2%	HP1262	NADH-ubiquinone oxidoreductase, NQO5 subunit (NQO5)	44.6%	<i>TCA cycle</i>		
HP1332	co-chaperone and heat-shock protein (dnaJ)	42.7%	HP1261	NADH-ubiquinone oxidoreductase, NQO6 subunit (NQO6)	-1.0%	HP0779	aconitase B (acnB)	64.0%
HP0110	co-chaperone and heat-shock protein (grpE)	33.0%	HP1260	NADH-ubiquinone oxidoreductase, NQO7 subunit (NQO7)	40.7%	HP0026	citrate synthase (gltA)	47.8%
HP1024	co-chaperone-curved DNA-binding protein A (CbpA)	37.7%	HP1267	NADH-ubiquinone oxidoreductase, NQO8 subunit (NQO8)	42.4%	HP1325	fumarase (fumC)	63.7%
<b>Chromosome-associated protein</b>						HP0509	glycolate oxidase subunit (gldC)	98.0%
HP1138	plasmid replication-partition related protein	40.4%	HP1268	NADH-ubiquinone oxidoreductase, NQO9 subunit (NQO9)	41.2%	HP0027	isocitrate dehydrogenase (icd)	70.7%
<b>Detoxification</b>						<b>FATTY ACID AND PHOSPHOLIPID METABOLISM</b>		
HP1563	alkyl hydroperoxide reductase (tsaA)	98.5%	<b>Amino acids and amines</b>			HP1376	(3R)-hydroxymyristoyl-acyl carrier protein dehydratase (fabZ)	47.4%
HP0875	catalase	99.4%	HP1398	alanine dehydrogenase (ald)	39.6%	HP1348	1-acylglycerol-3-phosphate acyltransferase (plsC) (Escherichia coli)	32.0%
HP0267	chlorohydrilase	42.6%	HP0294	aliphatic amidase (aimE)	75.4%	HP0561	3-ketoacyl-acyl carrier protein reductase (fabG)	45.7%
HP0243	neutrophil activating protein (napA) (bacterioferritin)	95.6%	HP1238	aliphatic amidase (aimE)	37.2%	HP0690	acetyl coenzyme A acetyltransferase (thioase) (fadA)	52.0%
HP0389	superoxide dismutase (sodB)	98.6%	HP1399	arginase (rocF)	31.8%	HP0950	acetyl-CoA carboxylase beta subunit (accD)	49.4%
HP1452	thiophene and furan oxidizer (tdhF)	37.6%	HP0943	D-amino acid dehydrogenase (dadA)	26.2%	HP1045	acetyl-CoA synthetase (accE)	52.3%
<b>Protein and peptide secretion</b>						HP0557	acetyl-coenzyme A carboxylase (accA)	50.3%
HP0355	GTP-binding membrane protein (lepA)	57.3%	HP0056	delta-1-pyrroline-5-carboxylate dehydrogenase (Synecocystis sp.)	32.2%	HP0559	acyl carrier protein (accP)	55.3%
HP0074	lipoprotein signal peptidase (lspA)	97.0%	HP0723	L-asparaginase II (ansB)	54.1%	HP0962	acyl carrier protein (accP)	56.3%
HP0786	preprotein translocase subunit (secA)	54.0%	HP0132	L-serine deaminase (sdaA)	45.8%	HP0558	beta ketoacyl-acyl carrier protein synthase II (fabF)	50.0%
HP1300	preprotein translocase subunit (secY)	41.2%	<b>Anaerobic</b>			HP0202	beta-ketoacyl-acyl carrier protein synthase III (fabH)	44.4%
HP1255	protein translocation protein, low temperature (secG)	30.6%	HP0666	anaerobic glycerol-3-phosphate dehydrogenase, subunit C (glpC)	27.2%	HP0371	biotin carboxyl carrier protein (fabE)	30.8%
HP1550	protein-export membrane protein (secD)	38.3%	HP0589	ferredoxin oxidoreductase, alpha subunit	42.7%	HP0370	biotin carboxylase (accC)	52.1%
HP1549	protein-export membrane protein (secE)	35.1%	HP0690	ferredoxin oxidoreductase, beta subunit	43.2%	HP0871	CDP-diglyceride hydrolase (cdh)	73.9%
HP0576	signal peptidase I (lepB)	40.3%	HP0591	ferredoxin oxidoreductase, gamma subunit	33.3%	HP0215	CDP-diglyceride synthetase (cdsA)	42.4%
HP1152	signal recognition particle protein (fih)	41.4%	HP0193	fumarate reductase, cytochrome b subunit (frcD)	58.8%	HP0416	cyclopropane fatty acid synthase (cfa)	39.7%
HP0795	trigger factor (tig)	27.6%	HP0192	fumarate reductase, flavoprotein subunit (frcA)	69.4%	HP0700	diacylglycerol kinase (dgaA)	45.8%
<b>Transformation</b>						HP0195	enoyl-acyl-carrier-protein reductase (NADH) (fabI)	45.8%
HP0620	cag pathogenicity island protein (cag1)	96.5%	HP0191	fumarate reductase, iron-sulfur subunit (frcB)	70.8%	HP0201	fatty acid/phospholipid synthesis protein (plsX)	37.8%
HP0530	cag pathogenicity island protein (cag10)	98.4%	HP1110	pyruvate ferredoxin oxidoreductase, alpha subunit	41.0%	HP0808	Holo-acp synthase (acpS)	29.1%
HP0531	cag pathogenicity island protein (cag11)	97.2%	HP1111	pyruvate ferredoxin oxidoreductase, beta subunit	43.7%	HP0900	malonyl coenzyme A-acyl carrier protein transacylase (fabD)	35.4%
HP0532	cag pathogenicity island protein (cag12)	98.9%	HP1109	pyruvate ferredoxin oxidoreductase, delta subunit	47.0%	HP1016	phosphatidylglycerophosphate synthase (pgsA)	35.4%
HP0534	cag pathogenicity island protein (cag13)	98.0%	HP1108	pyruvate ferredoxin oxidoreductase, gamma subunit	37.2%	HP1357	phosphatidylserine decarboxylase proenzyme (psd)	33.2%
HP0535	cag pathogenicity island protein (cag14)	97.6%	<b>ATP-protonmotive force interconversion</b>			HP1071	phosphatidylserine synthase (psaA)	99.6%
HP0536	cag pathogenicity island protein (cag15)	98.4%	HP0828	ATP synthase FO, subunit a (atpB)	37.7%	HP0499	phospholipase A1 precursor (DR-phospholipase A)	33.8%
HP0537	cag pathogenicity island protein (cag16)	98.9%	HP1136	ATP synthase FO, subunit b (atpF)	28.3%	<b>PURINES, PYRIMIDINES, NUCLEOSIDES AND NUCLEOTIDES</b>		
HP0538	cag pathogenicity island protein (cag17)	95.3%	HP1137	ATP synthase FO, subunit b0 (atpF0)	32.5%	<i>General</i>		
HP0539	cag pathogenicity island protein (cag18)	98.7%	HP1212	ATP synthase F1, subunit alpha (atpA)	41.2%	HP0757	beta-alanine synthetase homologue	40.0%
HP0540	cag pathogenicity island protein (cag19)	99.5%	HP1134	ATP synthase F1, subunit beta (atpD)	62.7%	<b>2'-Deoxyribonucleotide metabolism</b>		
HP0521	cag pathogenicity island protein (cag2)	92.5%	HP1132	ATP synthase F1, subunit beta (atpD)	85.6%	HP0372	deoxycytidine triphosphate deaminase (dcd)	28.2%
HP0541	cag pathogenicity island protein (cag20)	97.8%	HP1135	ATP synthase F1, subunit delta (atpH)	24.6%	HP0865	deoxyuridine 5'-triphosphate nucleotidohydrolase (dut)	41.4%
HP0542	cag pathogenicity island protein (cag21)	97.9%	HP1131	ATP synthase F1, subunit epsilon (atpC)	32.7%	HP0364	ribonucleoside diphosphate reductase, beta subunit (nrdB)	39.0%
HP0543	cag pathogenicity island protein (cag22)	95.5%	HP1133	ATP synthase F1, subunit epsilon (atpC)	37.8%	HP0680	ribonucleoside-diphosphate reductase 1 alpha subunit (nrDA)	28.4%
HP0544	cag pathogenicity island protein (cag23)	99.0%	<b>Electron transport</b>			HP0825	thioredoxin reductase (trxB)	45.9%
HP0545	cag pathogenicity island protein (cag24)	98.5%	HP0146	cb3-type cytochrome c oxidase subunit O (CooO)	44.2%	<b>Purine ribonucleotide biosynthesis</b>		
HP0546	cag pathogenicity island protein (cag25)	95.7%	HP0265	cytochrome c biogenesis protein (ccdA)	35.4%	HP0321	5'-guanylate kinase (gmk)	44.8%
HP0547	cag pathogenicity island protein (cag26)	92.9%	HP0378	cytochrome c biogenesis protein (lycF)	37.5%	HP0618	adenylate kinase (ack)	33.3%
HP0522	cag pathogenicity island protein (cag3)	98.1%	HP0147	cytochrome c oxidase, heme subunit, membrane-bound (f1xP)	33.0%	HP1112	adenylosuccinate lyase (purB)	49.5%
HP0523	cag pathogenicity island protein (cag4)	95.7%	HP0144	cytochrome c oxidase, heme b and copper-binding subunit, membrane-bound (f1xN)	43.9%	HP0255	adenylosuccinate synthetase (purA)	44.6%
HP0524	cag pathogenicity island protein (cag5)	99.1%	HP0145	cytochrome c oxidase, monoheme subunit, membrane-bound (f1xO)	45.7%	HP1434	formyltetrahydrofolate hydrolase (purU)	49.1%
HP0525	cag pathogenicity island protein (cag6)	97.5%	HP1461	cytochrome c551 peroxidase	48.5%	HP1218	glycinamide ribonucleotide synthetase (purD)	31.8%
HP0527	cag pathogenicity island protein (cag7)	94.6%	HP1227	cytochrome c553	38.4%	HP0854	GMP reductase (guaC)	31.8%
HP0528	cag pathogenicity island protein (cag8)	99.0%	HP0277	ferredoxin	52.5%	HP0409	GMP synthase (guaA)	56.1%
HP0529	cag pathogenicity island protein (cag9)	98.9%	HP0588	ferredoxin-like protein	42.6%	HP0829	inosine-5'-monophosphate dehydrogenase (guaB)	58.5%
HP1378	competence lipoprotein (comL)	25.5%	HP1508	ferredoxin-like protein	29.4%	HP0198	nucleoside diphosphate kinase (ndk)	67.7%
HP1361	competence locus E (comE3)	26.7%	HP1161	flavodoxin (fldA)	47.0%	HP0742	phosphoribosylpyrophosphate synthetase (prsA)	66.5%
HP1006	conjugal transfer protein (traG)	27.3%	HP0642	NAD(P)H-flavin oxidoreductase	46.1%	HP1530	purine nucleoside phosphorylase (punB)	20.7%
HP1421	conjugative transfer regulon protein (trbB)	30.7%	HP0954	oxygen-insensitive NAD(P)H nitroreductase	32.7%	<b>Pyrimidine ribonucleotide biosynthesis</b>		
HP0533	DNA processing chain A (dprA)	32.9%	HP0634	quinone-reactive Ni/Fe hydrogenase (hydD)	54.7%	HP1084	aspartate transcarbamoylase (pyrB)	38.7%
HP0042	trb1 protein	31.4%	HP0633	quinone-reactive Ni/Fe hydrogenase, cytochrome b subunit (hydC)	51.4%	HP0919	carbamoyl-phosphate synthase (glutamine-hydrolysing) (pyrAb)	48.6%
HP0525	VirB11 homologue	100.0%	HP0632	quinone-reactive Ni/Fe hydrogenase, large subunit (hydB)	68.5%	HP1237	carbamoyl-phosphate synthetase (pyrAa)	39.7%
HP0441	VirB4 homologue	23.5%	HP1539	ubiquinol cytochrome c oxidoreductase, cytochrome b subunit (fbcH)	39.3%	HP0349	GTP synthetase (pyrG)	50.7%
HP0017	virB4 homologue (virB4)	25.2%	HP1538	ubiquinol cytochrome c oxidoreductase, cytochrome c1 subunit (fbcH)	28.8%	HP0266	dihydroorotase (pyrC)	-1.0%
HP0459	virB4 homologue (virB4)	25.3%	HP1540	ubiquinol cytochrome c oxidoreductase, Rieske 2Fe-2S subunit (fbcF)	39.2%	HP0581	dihydroorotase (pyrC)	31.5%
<b>CENTRAL INTERMEDIARY METABOLISM</b>						HP1011	dihydroorotate dehydrogenase (pyrD)	41.5%
<i>General</i>						HP1257	orotate phosphoribosyltransferase (pyrE)	35.5%
HP1014	7- $\alpha$ -hydroxysteroid dehydrogenase (hdhA)	33.2%	<b>Enter-Doudoroff</b>			HP0005	orotidine 5'-phosphate decarboxylase (pyrF)	39.0%
HP1186	carbonic anhydrase	37.0%	HP1099	2-keto-3-deoxy-6-phosphogluconate aldolase (eda)	50.3%	HP1474	thymidylate kinase (tmk)	33.9%
HP0004	carbonic anhydrase (icfA)	33.3%	HP1100	6-phosphogluconate dehydratase	50.7%	HP0777	uridine 5'-monophosphate (UMP) kinase (pyrH)	50.4%
HP0869	hydrogenase expression/formation protein (hypA)	28.1%	<b>Fermentation</b>			<b>Salvage of nucleosides and nucleotides</b>		
HP0900	hydrogenase expression/formation protein (hypB)	41.4%	HP0691	3-oxoadipate coA-transferase subunit A (yxjD)	65.5%	HP1014	2,3-cyclic-nucleotide 2'-phosphodiesterase (cpdB)	31.8%
HP0899	hydrogenase expression/formation protein (hypC)	38.5%	HP0692	3-oxoadipate coA-transferase subunit B (yxjE)	73.2%	HP0672	adenine phosphoribosyltransferase (apt)	50.3%
HP0898	hydrogenase expression/formation protein (hypD)	47.8%	HP0903	acetate kinase (ackA) (Escherichia coli)	42.3%	HP1179	phosphopentomutase (deoB)	55.9%
HP0047	hydrogenase expression/formation protein (hypE)	39.7%	HP0904	phosphate acetyltransferase (pta)	51.0%	HP1178	purine-nucleoside phosphorylase (deoD)	55.5%
HP0197	S-adenosylmethionine synthetase 2 (metX)	62.1%	HP0905	phosphotransacetylase (pta)	26.9%	HP0735	xanthine guanine phosphoribosyl transferase (gpt)	27.1%
<b>Amino sugars</b>						<b>Sugar-nucleotide biosynthesis and conversions</b>		
HP1532	glucosamine fructose-6-phosphate aminotransferase (isomerizing) (glmS)	41.7%	HP0357	short-chain alcohol dehydrogenase	57.6%	HP0043	mannose-6-phosphate isomerase (pmi) or (algA)	42.8%
<b>Phosphorus compounds</b>						HP0045	modulation protein (nolK)	44.3%
HP0620	inorganic pyrophosphatase (ppa)	50.0%	<b>Gluconogenesis</b>			HP0646	UDP-glucose pyrophosphorylase (galU)	65.8%
HP0696	N-methylglutaminase	26.9%	HP1385	fructose-1,6-bisphosphatase	36.4%	HP0683	UDP-N-acetylglucosamine pyrophosphorylase (glmU)	40.0%
HP1010	polyphosphate kinase (ppk)	38.5%	HP0121	phosphoenolpyruvate synthase (ppsA)	52.4%	<b>REGULATORY FUNCTIONS</b>		
<b>Polyamine biosynthesis</b>						<i>General</i>		
HP0422	arginine decarboxylase (speA)	33.3%	HP1345	phosphoglycerate kinase	47.3%	HP1032	alternative transcription initiation factor, sigma-F (flaA)	34.6%
HP0020	carboxynorspermidine decarboxylase (nspC)	45.6%	HP0154	enolase (eno)	56.9%	HP1168	carbon starvation protein (cstA)	59.8%
HP0832	spermidine synthase (speE)	26.5%	HP0176	fructose-bisphosphate aldolase (tsr)	46.0%	HP1442	carbon storage regulator (csrA)	43.3%
<b>Other</b>						HP1027	ferric uptake regulation protein (fur)	39.9%
HP0070	urease accessory protein (ureE)	97.1%	HP1103	glucokinase (glk)	41.5%	HP0278	guanosine pentaphosphate phosphorylase (gppA)	26.4%
HP0069	urease accessory protein (ureF)	94.5%	HP1166	glucose-6-phosphate isomerase (pgi)	53.3%	HP0400	penicillin tolerance protein (lytB)	30.6%
HP0068	urease accessory protein (ureG)	95.0%	HP0921	glyceraldehyde-3-phosphate dehydrogenase (gap)	46.5%			
HP0067	urease accessory protein (ureH)	96.2%	HP1346	glyceraldehyde-3-phosphate dehydrogenase (gap)	46.7%			
HP0071	urease accessory protein (ureI)	98.5%	HP0974	phosphoglycerate mutase (pgm)	44.6%			
HP0073	urease alpha subunit (ureA)	100.0%	HP0194	triosephosphate isomerase (tpi)	34.5%			
HP0072	urease beta subunit (urea amidohydrolase) (ureB)	100.0%	<b>Pentose phosphate pathway</b>					
HP0075	urease protein (ureC)	98.0%	HP1386	D-ribulose-5-phosphate 3 epimerase (rpe)	44.2%			
<b>ENERGY METABOLISM</b>								
<i>Aerobic</i>								
HP1222	D-lactate dehydrogenase (ldd)	27.0%	HP1102	glucose-6-phosphate 1-dehydrogenase				
HP0961	glycerol-3-phosphate dehydrogenase (NAD(P)H)	36.8%						
HP0037	NADH-ubiquinone oxidoreductase subunit	19.4%						
HP1269	NADH-ubiquinone oxidoreductase, NQO10							



<i>Cations</i>							
HP0791	cadmium-transporting ATPase, P-type (caca)		HP0268	conserved hypothetical integral membrane protein	32.7%	HP0728	conserved hypothetical protein
HP0969	cation efflux system protein (czcA)	97.5%	HP0284	conserved hypothetical integral membrane protein	29.2%	HP0734	conserved hypothetical protein
HP1328	cation efflux system protein (czcA)	28.9%	HP0362	conserved hypothetical integral membrane protein	28.8%	HP0745	conserved hypothetical protein
HP1329	cation efflux system protein (czcA)	31.3%	HP0415	conserved hypothetical integral membrane protein	44.4%	HP0747	conserved hypothetical protein
HP1503	cation-transporting ATPase, P-type (copA)	93.9%	HP0467	conserved hypothetical integral membrane protein	100.0%	HP0760	conserved hypothetical protein
HP1073	copper ion binding protein (copP)	92.4%	HP0571	conserved hypothetical integral membrane protein	29.5%	HP0810	conserved hypothetical protein
HP1072	copper-transporting ATPase, P-type (copA)	93.9%	HP0644	conserved hypothetical integral membrane protein	30.3%	HP0813	conserved hypothetical protein
HP0471	glutathione-regulated potassium-efflux system protein (kefB)	93.3%	HP0677	conserved hypothetical integral membrane protein	28.5%	HP0823	conserved hypothetical protein
HP0687	iron(II) transport protein (fecB)	33.6%	HP0693	conserved hypothetical integral membrane protein	46.7%	HP0860	conserved hypothetical protein
HP1561	iron(III) ABC transporter, periplasmic iron-binding protein (ceuE)	27.5%	HP0718	conserved hypothetical integral membrane protein	33.5%	HP0890	conserved hypothetical protein
HP1562	iron(III) ABC transporter, periplasmic iron-binding protein (ceuE)	28.2%	HP0737	conserved hypothetical integral membrane protein	33.3%	HP0891	conserved hypothetical protein
HP0888	iron(III) diclolate ABC transporter, ATP-binding protein (fecC)	34.4%	HP0758	conserved hypothetical integral membrane protein	47.6%	HP0892	conserved hypothetical protein
HP0889	iron(III) diclolate ABC transporter, permease protein (fecD)	38.3%	HP0759	conserved hypothetical integral membrane protein	31.1%	HP0894	conserved hypothetical protein
HP0886	iron(III) diclolate transport protein (fecA)	29.7%	HP0787	conserved hypothetical integral membrane protein	25.2%	HP0926	conserved hypothetical protein
HP0807	iron(III) diclolate transport protein (fecA)	28.5%	HP0851	conserved hypothetical integral membrane protein	37.3%	HP0934	conserved hypothetical protein
HP1400	iron(III) diclolate transport protein (fecA)	26.3%	HP0920	conserved hypothetical integral membrane protein	36.3%	HP0956	conserved hypothetical protein
HP1344	magnesium and cobalt transport protein (corA)	26.3%	HP0946	conserved hypothetical integral membrane protein	35.9%	HP0959	conserved hypothetical protein
HP1183	Na <sup>+</sup> /H <sup>+</sup> antiporter (napA)	26.6%	HP0962	conserved hypothetical integral membrane protein	38.5%	HP0966	conserved hypothetical protein
HP1552	Na <sup>+</sup> /H <sup>+</sup> antiporter (nhaA)	49.2%	HP0983	conserved hypothetical integral membrane protein	32.8%	HP0975	conserved hypothetical protein
HP1077	nickel-transport protein (nixA)	98.7%	HP1044	conserved hypothetical integral membrane protein	30.6%	HP1020	conserved hypothetical protein
HP0490	putative potassium channel protein, putative	25.7%	HP1061	conserved hypothetical integral membrane protein	35.0%	HP1037	conserved hypothetical protein
<i>Nucleosides, purines and pyrimidines</i>			HP1080	conserved hypothetical integral membrane protein	44.0%	HP1046	conserved hypothetical protein
HP1290	nicotinamide mononucleotide transporter (pnuC)	28.0%	HP1162	conserved hypothetical integral membrane protein	27.6%	HP1049	conserved hypothetical protein
HP1180	pyrimidine nucleoside transport protein (nupC)	32.9%	HP1175	conserved hypothetical integral membrane protein	40.6%	HP1066	conserved hypothetical protein
<i>Other</i>			HP1184	conserved hypothetical integral membrane protein	23.5%	HP1149	conserved hypothetical protein
HP0876	iron-regulated outer membrane protein (frpB)	27.6%	HP1185	conserved hypothetical integral membrane protein	55.5%	HP1160	conserved hypothetical protein
HP0915	iron-regulated outer membrane protein (frpB)	28.1%	HP1225	conserved hypothetical integral membrane protein	31.6%	HP1162	conserved hypothetical protein
HP0916	iron-regulated outer membrane protein (frpB)	28.8%	HP1234	conserved hypothetical integral membrane protein	29.0%	HP1124	conserved hypothetical protein
HP1129	biopolymer transport protein (exbD)	29.7%	HP1235	conserved hypothetical integral membrane protein	30.9%	HP1128	conserved hypothetical protein
HP1130	biopolymer transport protein (exbB)	33.5%	HP1330	conserved hypothetical integral membrane protein	41.7%	HP1133	conserved hypothetical protein
HP1339	biopolymer transport protein (exbB)	46.8%	HP1331	conserved hypothetical integral membrane protein	33.6%	HP1137	conserved hypothetical protein
HP1340	biopolymer transport protein (exbD)	35.8%	HP1343	conserved hypothetical integral membrane protein	49.1%	HP1138	conserved hypothetical protein
HP1445	biopolymer transport protein (exbB)	45.5%	HP1363	conserved hypothetical integral membrane protein	33.1%	HP1139	conserved hypothetical protein
HP1446	biopolymer transport protein (exbD)	36.2%	HP1407	conserved hypothetical integral membrane protein	22.4%	HP1141	conserved hypothetical protein
HP1512	iron-regulated outer membrane protein (frpB)	26.6%	HP1466	conserved hypothetical integral membrane protein	30.9%	HP1144	conserved hypothetical protein
HP0653	nonheme iron-containing ferritin (pfr)	99.4%	HP1484	conserved hypothetical integral membrane protein	41.2%	HP1147	conserved hypothetical protein
HP1341	siderophore-mediated iron transport protein (tonB)	37.2%	HP1486	conserved hypothetical integral membrane protein	23.8%	HP1149	conserved hypothetical protein
<i>OTHER CATEGORIES</i>			HP1487	conserved hypothetical integral membrane protein	30.7%	HP1150	conserved hypothetical protein
<i>General</i>			HP1509	conserved hypothetical integral membrane protein	34.3%	HP1151	conserved hypothetical protein
HP0924	4-oxalocrotonate tautomerase (dmpl)	37.7%	HP1548	conserved hypothetical integral membrane protein	30.6%	HP1126	conserved hypothetical protein
HP1034	ATP-binding protein (ylxH)	36.3%	HP0138	conserved hypothetical iron-sulfur protein	41.2%	HP1285	conserved hypothetical protein
HP1000	PARA protein	23.7%	HP1438	conserved hypothetical lipoprotein	32.0%	HP1286	conserved hypothetical protein
HP1139	SpoCJ regulator (soj)	47.4%	HP0151	conserved hypothetical membrane protein	21.8%	HP1464	conserved hypothetical protein
HP0827	ss-DNA binding protein 12RNP2 precursor	46.8%	HP0575	conserved hypothetical membrane protein	38.8%	HP1488	conserved hypothetical protein
<i>Adaptations and atypical conditions</i>			HP1258	conserved hypothetical mitochondrial protein 4	23.2%	HP1551	conserved hypothetical secreted protein
HP1496	general stress protein (ctc)	26.5%	HP1492	conserved hypothetical niuH-like protein	48.2%	HP0028	conserved hypothetical secreted protein
HP1483	gerC2 protein (gerC2)	33.3%	HP0032	conserved hypothetical protein	37.0%	HP0139	conserved hypothetical secreted protein
HP0927	heat shock protein (hspX)	32.8%	HP0035	conserved hypothetical protein	34.1%	HP0160	conserved hypothetical secreted protein
HP0280	heat shock protein B (hspB)	27.2%	HP0086	conserved hypothetical protein	26.7%	HP0190	conserved hypothetical secreted protein
HP1228	invasion protein (invA)	38.2%	HP0094	conserved hypothetical protein	29.8%	HP0211	conserved hypothetical secreted protein
HP0970	nickel-cobalt-cadmium resistance protein (nccB)	21.1%	HP0102	conserved hypothetical protein	32.0%	HP0235	conserved hypothetical secreted protein
HP1444	small protein (smpB)	42.1%	HP0105	conserved hypothetical protein	39.7%	HP0257	conserved hypothetical secreted protein
HP0930	stationary-phase survival protein (surE)	37.7%	HP0117	conserved hypothetical protein	34.2%	HP0320	conserved hypothetical secreted protein
HP0315	virulence associated protein D (vapD)	70.2%	HP0162	conserved hypothetical protein	36.7%	HP0506	conserved hypothetical secreted protein
HP0967	virulence associated protein D (vapD)	28.9%	HP0216	conserved hypothetical protein	33.9%	HP0518	conserved hypothetical secreted protein
HP1248	virulence associated protein homolog (vacB)	36.0%	HP0233	conserved hypothetical protein	30.5%	HP0785	conserved hypothetical secreted protein
HP0886	virulence factor mviN protein (mviN)	33.5%	HP0248	conserved hypothetical protein	30.7%	HP0949	conserved hypothetical secreted protein
<i>Colicin-related functions</i>			HP0274	conserved hypothetical protein	38.5%	HP0977	conserved hypothetical secreted protein
HP1126	colicin tolerance-like protein (tolB)	25.7%	HP0285	conserved hypothetical protein	30.8%	HP0980	conserved hypothetical secreted protein
HP0428	phage/colicin/tellurite resistance cluster terY protein	25.6%	HP0309	conserved hypothetical protein	31.3%	HP1075	conserved hypothetical secreted protein
<i>Drug and analog sensitivity</i>			HP0310	conserved hypothetical protein	33.7%	HP1098	conserved hypothetical secreted protein
HP1431	16S rRNA (adenosine-N6,N6)-dimethyltransferase (kgpA)	35.5%	HP0318	conserved hypothetical protein	47.2%	HP1117	conserved hypothetical secreted protein
HP0606	membrane fusion protein (mtrC)	24.2%	HP0328	conserved hypothetical protein	30.7%	HP1216	conserved hypothetical secreted protein
HP0830	modulator of drug activity (mda68)	62.3%	HP0334	conserved hypothetical protein	30.8%	HP1285	conserved hypothetical secreted protein
HP1476	phenylacrylic acid decarboxylase	39.7%	HP0347	conserved hypothetical protein	31.8%	HP1464	conserved hypothetical secreted protein
HP1165	tetracycline resistance protein tet(A), putative	27.0%	HP0373	conserved hypothetical protein	31.4%	HP1488	conserved hypothetical secreted protein
<i>Transposon-related functions</i>			HP0374	conserved hypothetical protein	24.7%	HP1551	conserved hypothetical secreted protein
HP1008	IS200 insertion sequence from SARA17	33.9%	HP0388	conserved hypothetical protein	39.8%	HP0028	conserved hypothetical secreted protein
HP0414	IS200 insertion sequence from SARA17	33.9%	HP0395	conserved hypothetical protein	39.9%	HP0139	conserved hypothetical secreted protein
HP0988	IS605 transposase (tnpA)	97.2%	HP0396	conserved hypothetical protein	33.7%	HP0160	conserved hypothetical secreted protein
HP0988	IS605 transposase (tnpA)	97.2%	HP0419	conserved hypothetical protein	46.6%	HP0190	conserved hypothetical secreted protein
HP1038	IS605 transposase (tnpA)	97.2%	HP0447	conserved hypothetical protein	38.2%	HP0211	conserved hypothetical secreted protein
HP1535	IS605 transposase (tnpA)	97.2%	HP0466	conserved hypothetical protein	95.9%	HP0235	conserved hypothetical secreted protein
HP0437	IS605 transposase (tnpA)	97.2%	HP0488	conserved hypothetical protein	97.1%	HP0257	conserved hypothetical secreted protein
HP0989	IS605 transposase (tnpB)	93.4%	HP0469	conserved hypothetical protein	95.1%	HP0320	conserved hypothetical secreted protein
HP0997	IS605 transposase (tnpB)	93.4%	HP0496	conserved hypothetical protein	99.2%	HP0506	conserved hypothetical secreted protein
HP1095	IS605 transposase (tnpB)	93.4%	HP0507	conserved hypothetical protein	37.2%	HP0518	conserved hypothetical secreted protein
HP1534	IS605 transposase (tnpB)	93.4%	HP0519	conserved hypothetical protein	95.3%	HP0785	conserved hypothetical secreted protein
HP0438	IS605 transposase-like protein, PS3IS	33.8%	HP0552	conserved hypothetical protein	37.6%	HP0949	conserved hypothetical secreted protein
HP1007	transposase-like protein, PS3IS	34.3%	HP0553	conserved hypothetical protein	30.0%	HP0977	conserved hypothetical secreted protein
<i>Other</i>			HP0639	conserved hypothetical protein	41.0%	HP0980	conserved hypothetical secreted protein
HP0739	2-hydroxy-6-oxohepta-2,4-dienoate hydrolase	30.1%	HP0654	conserved hypothetical protein	32.0%	HP1075	conserved hypothetical secreted protein
<i>HYPOTHETICAL</i>			HP0656	conserved hypothetical protein	36.0%	HP1098	conserved hypothetical secreted protein
<i>General</i>			HP0707	conserved hypothetical protein	40.1%	HP1117	conserved hypothetical secreted protein
HP0831	conserved hypothetical ATP binding protein	32.3%	HP0709	conserved hypothetical protein	49.6%	HP1216	conserved hypothetical secreted protein
HP0066	conserved hypothetical ATP-binding protein	34.7%	HP0710	conserved hypothetical protein	33.7%	HP1285	conserved hypothetical secreted protein
HP0269	conserved hypothetical ATP-binding protein	37.7%	HP0716	conserved hypothetical protein	30.2%	HP1464	conserved hypothetical secreted protein
HP0312	conserved hypothetical ATP-binding protein	34.1%				HP1488	conserved hypothetical secreted protein
HP1321	conserved hypothetical ATP-binding protein	30.8%				HP1551	conserved hypothetical secreted protein
HP1430	conserved hypothetical ATP-binding protein	33.1%				UNKNOWN	
HP1507	conserved hypothetical ATP-binding protein	51.6%				<i>General</i>	
HP1567	conserved hypothetical ATP-binding protein	40.9%				HP0390	adhesin-thiol peroxidase (tagD)
HP1026	conserved hypothetical helicase-like protein	35.2%				HP1193	aldo-keto reductase, putative
HP0022	conserved hypothetical integral membrane protein	30.8%				HP0872	alkylphosphonate uptake protein (pfnA)
HP0189	conserved hypothetical integral membrane protein	43.1%				HP0136	bacterioferritin comigratory protein (bcp)
HP0226	conserved hypothetical integral membrane protein	27.6%				HP0485	catalase-like protein
HP0228	conserved hypothetical integral membrane protein	43.2%				HP1104	cinnamyl-alcohol dehydrogenase ELI3-2 (cad)
HP0234	conserved hypothetical integral membrane protein	32.4%				HP0981	exonuclease VII-like protein (xseA)
						HP0659	GTP-binding protein (gtp1)
						HP0303	GTP-binding protein (obg)
						HP0334	GTP-binding protein homologue (yphC)
						HP0480	GTP-binding protein, fusa-homolog (yihK)
						HP1489	lipase-like protein
						HP0405	niif-like protein
						HP0221	niuf-like protein
						HP0658	PET112-like protein
						HP0089	pfs protein (pfs)
						HP0322	poly E-rich protein
						HP0625	protein E (gpcE)
						HP0431	protein phosphatase 2C homolog (ptc1)
						HP0624	solute-binding signature and mitochondrial signature protein (aspB)
						HP0377	thioisulfide interchange protein (dsbC), putative